



Tectonics and volcanism in East Asia: Insights from geophysical observations



YoungHee Kim ^a, Changyeol Lee ^b, Seung-Sep Kim ^{c,*}

^aSchool of Earth and Environment Sciences, Seoul National University, Seoul 151-742, South Korea

^bFaculty of Earth and Environmental Sciences, Chonnam National University, Gwangju 500-757, South Korea

^cDepartment of Geology and Earth Environmental Sciences, Chungnam National University, Daejeon 305-764, South Korea

ARTICLE INFO

Article history:

Received 4 March 2015

Received in revised form 15 July 2015

Accepted 30 July 2015

Available online 31 July 2015

Keywords:

Intraplate volcanism

Subduction

Adakites

East Asia

Jeju Island

Lithospheric structure

ABSTRACT

We review geophysical and geochemical properties in the vicinity of the stagnant Pacific slab beneath northeast China, Korea and Japan to understand the origin and current state of intraplate volcanism in East Asia. East Asia has been susceptible to intensive volcanism since the Cretaceous. In particular, during the Cenozoic, Jeju Island, Korea is the most significant volcanic construct in East Asia. The generation of adakites and A-type granitoids littered throughout East Asia during the Cretaceous has been previously explained by the subduction of the Izanagi–Pacific ridge system. However, a recently revised plate reconstruction model does not comprise such a tectonic episode and consequently fails to explain adakites in arc magmatism during the Cretaceous. Thus, we propose an alternative hypothesis: temporal plume–slab interaction on the source of East Asian magmatism in order to trigger the adakites in arc magmatism without ridge subduction. In addition, we provide an overview on the tectonics and volcanism of Jeju Island during the Cenozoic in the context of the lithospheric structure from seismological constraints and recent geochemical results. The main scientific aims are to understand the consequences of mantle mixing in response to long-term subduction and subsequent changes on the stress state to determine the distribution of chemical heterogeneities, and thus define the origin and development of intraplate volcanism in East Asia. Although geophysical and geochemical data for Jeju Island are not sufficient at present, we strongly state that Jeju Island and the surrounding regions hold a key to unraveling the source of intraplate magmatism since the Cretaceous.

© 2015 Elsevier Ltd. All rights reserved.

1. Introduction

The subduction zone process operating over much of the Earth's history induces long-term mantle mixing and chemical heterogeneity and recycles volatiles into the mantle (Stixrude and Lithgow-Bertelloni, 2012, and references therein). Arc systems may hold the key for resolving the mystery of mass and heat transport in the Earth's mantle and the composition of the Earth's interior (Schubert et al., 2001). We have examined structural and magmatic properties in the vicinity of the stagnant Pacific slab beneath northeast China, Korea and Japan (Fig. 1) to define the role of mantle mixing in the presence of current and past subduction, and to understand the origin of intraplate volcanism.

* Corresponding author at: Geology and Earth Environmental Sciences, Chungnam National University, 99 Daehak-ro, Yuseong-gu, Daejeon 305-764, South Korea.

E-mail addresses: younghkim@snu.ac.kr (Y. Kim), changyeol.lee@gmail.com (C. Lee), seungsep@cnu.ac.kr (S.-S. Kim).

The Pacific slab penetrating down to the 410 km discontinuity and lying flat on the 660 km discontinuity beneath Japan, Korea, and China has been imaged seismically (e.g., Bijwaard et al., 1998; Huang and Zhao, 2006; Li et al., 2008; Fukao et al., 2009; Wei et al., 2012). The Pacific slab's presence in the mantle transition zone has been widely accepted in the Earth Science community. These seismic images suggest that the active intraplate volcanoes (located ~1000 km away from the Japan Trench) in East Asia do not have a hotspot origin, but might be closely related to the subduction process of the Pacific slab (e.g., Tang et al., 2014). Slower P- and S-wave velocity anomalies in the back-arc region are used to explain the source of the back-arc magmatism and to infer the convective circulation process of the mantle wedge (Zhao, 2012, and references therein). Geochemical studies also support the influence of the slab in the volcanism (Kuritani et al., 2011).

The presence of the Pacific slab in the mantle depth signifies that East Asian tectonics is in the broad deformation zone. Deep slab subduction has influenced seismic and volcanic activities in the region. However, its relationship to the magmatism in oceanic

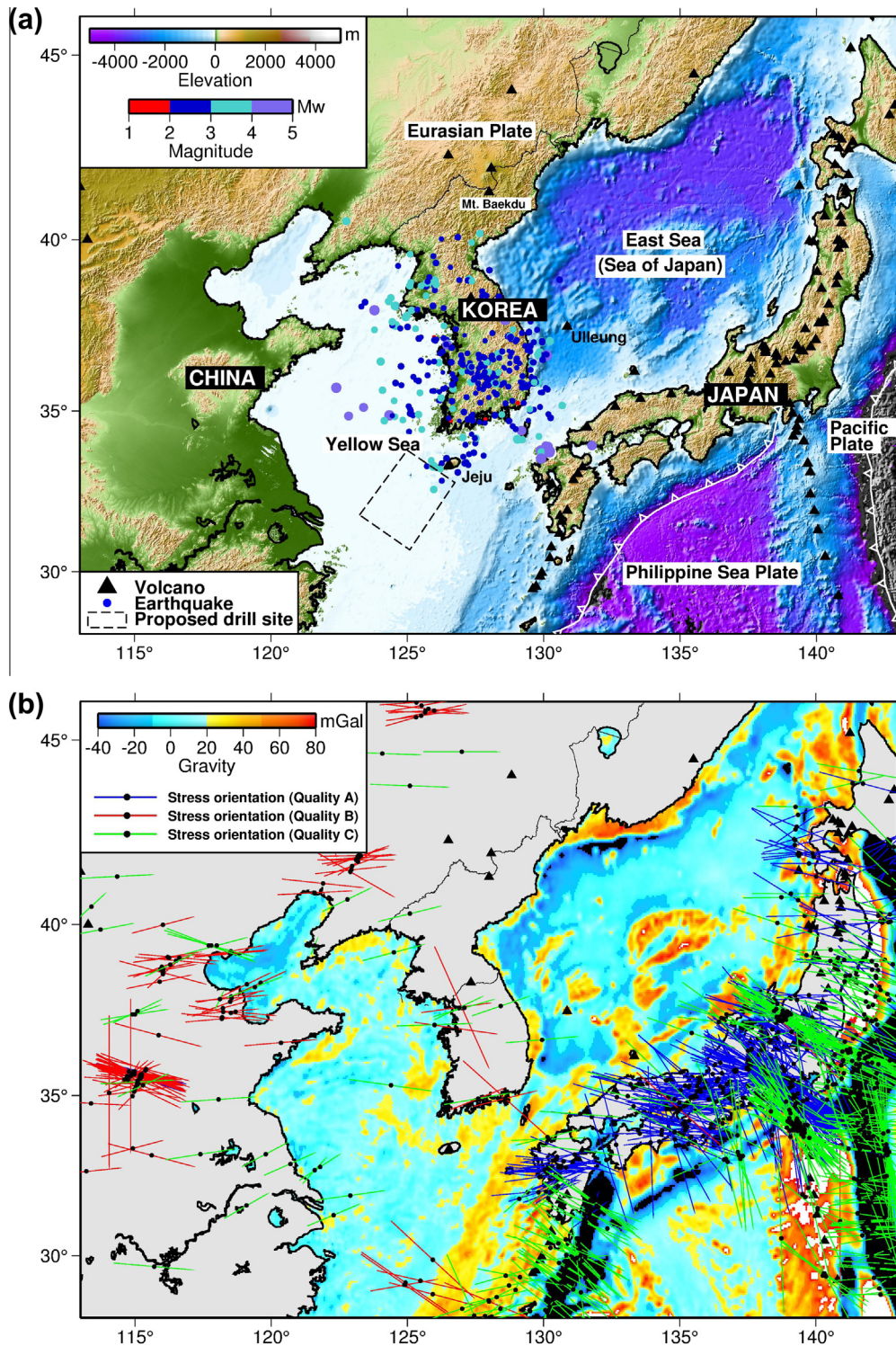


Fig. 1. Geophysical datasets probing East Asia. Locations of volcanoes are shown as black triangles in all panels (a and b). (a) Topographic-bathymetric map showing the region of study and regional seismic activities (colored circles) between 2001 and 2007. The size of the circles is proportional to the magnitude of the earthquake. (b) Gravity anomaly (Sandwell and Smith, 2009; Sandwell et al., 2013, 2014) and tectonic stress orientation in East Asia (Heidbach et al., 2008). Higher quality estimates (qualities A–C) on the stress vector are plotted. 'A' quality means that the orientation of maximum horizontal compressional stress (S_H) is accurate within $\pm 15^\circ$. 'B' quality is accurate within $\pm 20^\circ$. 'C' quality is accurate within $\pm 25^\circ$. Negative gravity anomalies are observed along the Japan Trench (shown as a white line with triangles in (a)). (For interpretation of the references to color in this figure legend, the reader is referred to the web version of this article.)

islands (Jeju and Ulleung; Fig. 1a) of Korea, coupled with an opening of the back-arc, remains unclear. Furthermore, physical mechanisms that have produced crustal extension, cratonic rejuvenation, and lithospheric thinning across parts of northeastern

China and their relationship to the subducted slab remain poorly understood.

Recent three-dimensional waveform modeling results from large-scale, high-density seismic arrays in northeastern China

(NECESS Array; Tang et al., 2014) suggest a new mechanism for intraplate volcanism of Mt. Baekdu (Changbai in Chinese; Fig. 1a). Tang et al. (2014) identifies a slow, continuous seismic anomaly from ~660 km depth to the surface beneath Mt. Baekdu, which has been occurring within a gap in the stagnant Pacific slab. This anomaly may represent hot and buoyant sub-lithospheric mantle that has been entrained beneath the sinking lithosphere and is now escaping through a gap in the subducting slab (Tang et al., 2014). Also, the subduction-induced upwelling process produces decompression melting that feeds the magmatism (Tang et al., 2014).

The absence of a long-tailed, stagnant slab beneath the chain of active volcanoes in northeastern China might suggest a possible link of volcanism either to the mantle transition zone or the lower mantle (Tang et al., 2014). Localized plume–slab interaction triggered by the slab tear can be modeled by numerical simulation. Recently, Lee and Lim (2014) have demonstrated the slab melting process by injecting a short-term temperature anomaly into the mantle wedge in order to explain pulse-like Abukuma adakites in northeastern Japan. They have suggested that such a short-term temperature anomaly can exist as a blob, which may have penetrated through a neck in the subducting Pacific slab.

Increasing geophysical observations and numerical capabilities have opened a new discussion on the origin of off-arc volcanism in a wider context of global geodynamics. This paper provides an opportunity to examine the magmatic process and tectonic evolution in East Asia since the Cretaceous and more importantly provides stronger constraints on the Cretaceous volcanism based on numerical simulation. Regardless of the scarcity of geophysical data, especially near Korea, we depict a more complete picture of how past and current subduction processes may introduce volatile and chemical heterogeneities into the mantle and trigger Cenozoic volcanism. We expect that these findings will provide the basis to discuss long-standing questions regarding the composition of the deep upper mantle and how it might be associated with large-scale mantle convection and mixing.

2. Cretaceous volcanism in East Asia

2.1. Tectonic models of the Cretaceous East Asia

The tectonics of East Asia including China, Korea, and Japan (Fig. 1) has been actively studied by many geoscientists for decades. The studies aim to clarify the source of volcanism since the Cretaceous. Numerical studies focus on Cretaceous tectonics and volcanisms in East Asia based on southwest-to-northeast migration of the peak (adakites and A-type granitoids) magmatism along southeast China, southeastern Korea, the Japanese Islands, and Kamchatka (Kinoshita, 1995; Maruyama et al., 1997) (Fig. 2a). Also, the numerical studies are from the following geological evidence: intraplate A-type granitoids in eastern and northeastern China (Wang et al., 2006; Wu et al., 2002, 2005); high-Mg basalts such as picrites in North China Craton (Gao et al., 2008); adakitic rocks in eastern China (Castillo, 2012; Wang et al., 2006; Xu et al., 2002); and the basin-and-range type fault basins such as Songliao, Bohaiwan and the North Yellow Sea basins in China and the Yellow Sea (Kim et al., 2012; Okada, 1999; Ren et al., 2002).

Two major tectonic episodes are suggested to explain the genesis of the diverse intraplate arc magmatism and the complex tectonic structures in East Asia. One tectonic episode is the southwest-to-northeast migration of the ridge subduction, which bounds the Izanagi and Pacific oceanic plates (Isozaki et al.,

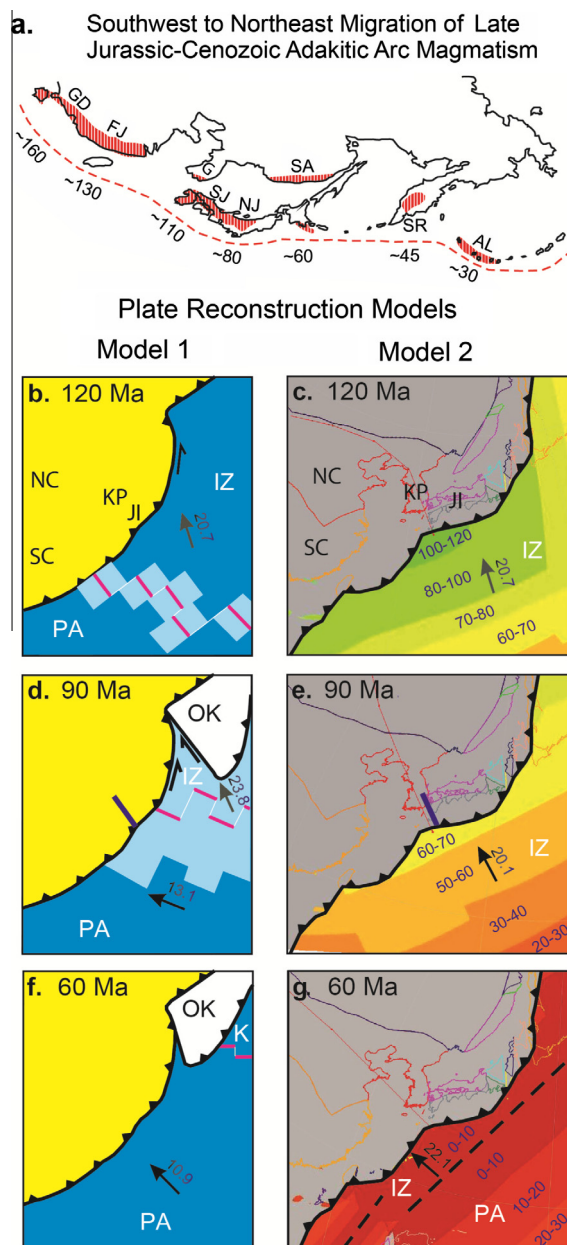


Fig. 2. Migration of peak magmatism (adakites and A-type granitoids) in East Asia during the Cretaceous and previously published two plate reconstruction models. (a) Southwest-to-northeast migration of the peak magmatism in East Asia during the Cretaceous (modified from Lee and Ryu, 2016). (b, d, and f) Plate reconstruction model 1 (Maruyama et al., 1997). Southwest-to-northeast migration of the mid-ocean ridge between the Pacific and Izanagi plates results in concurrent arc magmatism in East Asia. NC, SC, KP, JI, PA, IZ, and OK represent North China, South China, Korean Peninsula, Japanese Islands, and the Pacific, Izanagi, and Okhotsk plates, respectively. (c, e, and g) Plate reconstruction model 2 (Sdrolias and Müller, 2006). The major difference with Model 1 is that ridge subduction did not occur in Model 2 during the entire Cretaceous, which poses a serious issue on the arc genesis.

2010; Kinoshita, 1995; Maruyama et al., 1997) (Model 1 in Figs. 2b, d, and f). The southwest-to-northeast ridge migration roughly proceed at a rate of 3.0 cm/yr and is essential for explaining the genesis of the concurrent migration of adakites and A-type granitoids along the ancient subduction zone (Kinoshita, 1995, 2002). The other tectonic episode is the upwelling of the hot asthenospheric mantle beneath the region of China (Gao et al., 2008; Menzies et al., 2007; Ren et al., 2002; Wang et al., 2006).

2.2. Issues in the current tectonic models during the Cretaceous

A recent plate reconstruction model (Model 2 in Fig. 2c, e, and g; Sdrolias and Müller, 2006) has undergone significant changes (Model 1 in Fig. 2b, d, and f). Several notable improvements are developed: back-arc basins formed in the Pacific and Indian margins (Gaina and Müller, 2007; Sdrolias and Müller, 2006), tectonic history of the Australian and Antarctic continents (Heine et al., 2004; Sokolov et al., 2002), and the continuous spreading of the Izanagi and Pacific ridge systems during the Cretaceous (Müller et al., 2008). A major difference between Models 1 and 2 (Fig. 2) is that the recent plate reconstruction model does not show any ridge subduction beneath East Asia during the entire Cretaceous. Thus, the genesis of the adakites cannot be explained with the revised model.

A recent numerical study by Lee and Ryu (2016) evaluates the effect of temporal subduction (e.g., evolving convergence rate and slab age) on the thermal structure of the subducting slab. In this study, they use two plate reconstruction models (Models 1 and 2; Fig. 2) based on time-evolving two-dimensional subduction model calculations. Lee and Ryu (2016) report that the ridge subduction between the Izanagi and Pacific plates in their model calculation yields higher temporal slab surface temperatures than the solidus of wet basalt. Lee and Ryu (2016) use this result to explain the partial melting of oceanic crust and subsequently the presence of the adakites in the Japanese Islands. However, the experiment excluding the ridge subduction does not show any partial melting of the crust, which poses a major issue on the genesis of adakites and A-type granitoids, and the southwest-to-northeast migration along the arc. Therefore, the new plate reconstruction model is not consistent with the southwest-to-northeast migration of the adakites along the Japanese Islands.

Although ridge subduction may be vital to explain the Cretaceous magmatism in Japan, it cannot fully explain the intraplate magmatism in China. First, adakitic rocks are broadly scattered across China and have higher $^{87}\text{Sr}/^{86}\text{Sr}$ and lower $^{143}\text{Nd}/^{144}\text{Nd}$ than typical adakites in Japan. This evidence implies that the genesis of adakitic rocks in China might not be directly related to the partial melting of subducting oceanic crust, but might come from other geologic and tectonic processes. Second, the locations of the adakitic rocks are too far from the ancient subduction zone (>1000 km).

High Mg basalts in China such as picrites require extreme mantle potential temperatures (>200 K higher than the ordinary mantle), which may imply the presence of anomalous heating process in back-arc mantle. Because the mantle is most likely under near adiabatic conditions, ascending mantle from the deeper mantle adiabatically loses its internal (heat) energy through adiabatic expansion (Schubert et al., 2001). The ascending asthenosphere cannot keep its heat energy up to the shallow mantle. Therefore, the mantle should be anomalously hotter than the ordinary mantle. These lines of unresolved issues indicate that the upwelling of hot asthenospheric mantle (Gao et al., 2008; Menzies et al., 2007; Ren et al., 2002; Wang et al., 2006) is not sufficient for diverse and complicated intraplate and arc magmatism.

3. Cenozoic volcanism in East Asia: Three candidate models

3.1. Active plume model

As shown in Fig. 1, the tectonic setting and the lithospheric structure of East Asia has been influenced greatly from the subduction of two oceanic plates (Pacific and Philippine Sea plates). Quaternary volcanism in northeastern Honshu Island, Japan is a clear example of subduction-related volcanism (Tatsumi et al.,

1983; Tatsumi and Nakano, 1984). However, Cenozoic magmatism from the subduction of such plates throughout East Asia, especially Korea, southwestern Japan, and northeastern China has not been clearly explained based upon physical and/or geochemical evidence.

Whereas the alkaline basalts from Korea and northeastern China do not have island arc signatures, Japanese basalts exhibit weak island arc signatures with K, Ba, and Rb enrichment and slight depletion in Ta relative to La (Nakamura et al., 1989). Such regional geochemical differences indicate that the magma source beneath southwestern Japan has been affected only by the dehydration of the subducting Pacific plate. Since the subducting Philippine Sea plate is located shallower than the Pacific plate as evidenced by seismic images (e.g., Huang et al., 2013; Long et al., 2007; Zhao et al., 2004), subduction of the Philippine Sea plate may not be associated with generating alkaline basaltic magmatism beneath southwestern Japan.

To explain the Cenozoic volcanism in Korea and northeastern China, Nakamura et al. (1989) suggest that the mantle plume may have reacted with the mid-ocean ridge basalts (MORB)-type mantle to produce alkaline basalt magma. In this perspective, Japanese basalts can be the results of plume interactions with weakly metasomatized MORB-type depleted mantle. Tatsumi et al. (2004) propose a more evolved plume model to explain the volcanic origin of Jeju Island. However, the absence of topographic swells and the age progression of volcanic lineaments prevent researchers from actively utilizing the plume model to understand the Cenozoic volcanism in East Asia.

3.2. Passive melting model

Another candidate model to explain the Cenozoic volcanic activity is passive rift decompression melting. This model is proposed from a series of geochemical analysis on several petrology samples in different localities. Thus, this geochemistry-based melting model appears to be heavily constrained by the geographic location of samples.

Similar to previous plume-supporting studies (e.g., Nakamura et al., 1989; Tatsumi et al., 2004), Chen et al. (2007) confirm no clear evidence of subducting slab components in the Cenozoic volcanism from the major and trace elements rooted from eleven volcanic fields in northeastern China. Furthermore, their data do not indicate any high- $^3\text{He}/^4\text{He}$ mantle plume component beneath northeastern China. Instead, they reexamine previously reported Sr-Nb-Pb isotopic data (Basu et al., 1991; Peng et al., 1986; Tu et al., 1992; Zhang et al., 1991; Zhou and Armstrong, 1982), and suggest mantle source originating from a mixing between FOZO end-member and LoMu end-member. The LoMu end-member appears to reside within the continental lithosphere. Chen et al. (2007) consider that highly potassic basalts can be associated with the LoMu end-member as a product of lithosphere melting.

However, based on the Sr, Nd, Pb, and Hf isotopic compositions from six late Cenozoic basaltic volcanic centers in Korea, Choi et al. (2006) disregard both existence of mantle plume and decompression melting of the mantle lithosphere in a rift environment as origins of the Cenozoic volcanism. They propose two different arrays of mantle sources beneath East Asia: a depleted mantle-enriched mantle 1 (DMM-EM1) array for northeastern China and a depleted mantle-enriched mantle 2 (DMM-EM2) array for southeastern Asia. Because of more basaltic components in samples from Korea, they associate Korean basalts with an array between DMM and an intermediate end member between EM1 and EM2. Furthermore, they observed systematic regional isotopic progression from most of southern Korea to western Korea. The EM2 signature is the most significant in Jeju Island whereas the EM1 component is predominant among Ulleung Island, Ganseong area,

and Baengnyeong Island (locations shown as stars in Fig. 3). Interestingly, such regional variations occur without any clear changes related in both basement crust and lithospheric mantle (Choi et al., 2006). Based on this observation, they propose that the Cenozoic volcanism resulted from a deeper source (i.e., asthenospheric mantle). Also, to explain asthenospheric melting by decompression, they suggest a possible interplay between the India–Eurasia collision (e.g., Gibbons et al., *in press*) and the subduction of the Pacific plate as a cause for the tensile tectonic setting in East Asia. However, it is not clear how temporal changes in tectonic stress regime induced by the India–Eurasia collision have been propagated to northeastern China, Korea and southwest Japan. Numerical studies reconstructing paleo-stresses illustrate that far-field plate boundary forces can be transmitted into heterogeneous plate interiors over thousands of kilometers (Dyksterhuis et al., 2005; Dyksterhuis and Müller, 2008; Liu et al., 2007). However, comprehensive assessment on geologic evidence due to changes in plate geometry and driving forces is limited by the complex interplay between juxtaposed geologic bodies with different continental rheology (Dyksterhuis and Müller, 2008; Liu et al., 2007).

3.3. Lithospheric-folding-based melting model

With a presence of tectonic compressional fields (indicated by stress vectors in Fig. 1b), lithospheric folding can be a standard mechanical response of the lithosphere. In order to explain the volcanic origin of Jeju Island, Shin et al. (2012) have proposed the lithospheric-folding model based on the inversion of gravity data. The horizontal force of the subducting Pacific plate is considered to be strong enough to buckle the lithosphere and ultimately trigger the decompression melting beneath the Island.

The lithospheric folding beneath Jeju Island might have resulted in a pressure decrease beneath the ridge of the fold while the pressure beneath the trough has increased (Shin et al., 2012). The decompression beneath the lithosphere is likely to cause basaltic magmatism along and below the ridge. However, such lithospheric folding may not be large enough to form a sizable volcano on Jeju Island. To ensure the longevity of the volcanism, Shin et al. (2012) suggest “episodic folding” as a cause in the instability of the mantle.

The lithospheric folding model by Shin et al. (2012) appears to be optimized for localized volcanism in Jeju only, and thus cannot explain widespread Cenozoic volcanism in East Asia. Furthermore, lithospheric deformation due to compressional force fields near Jeju is not clearly observed, and the correlation between the lithospheric folding near the southern part of Korea and the horizontal force of the subducting Pacific slab is weak. Based on this hypothesis, intraplate basaltic magmatism can be generated in the back-arc region without the presence of significant extensional tectonic force in East Asia. This is quite conflicting to the previous geochemically derived models (e.g., Chen et al., 2007; Choi et al., 2006), which greatly favors tectonic extensional force in East Asia.

4. Present-day lithospheric structure in East Asia

Continuous deployment of dense portable and permanent seismic arrays on continents and the ocean floor provides critical observations of the present-day lithospheric structure. The regional seismological datasets are used to identify the location and magnitude of seismic discontinuities separating regions of differing seismic impedance. These critical observables can be retrieved from a well-known technique in travel-time tomography (e.g., Rawlinson et al., 2010; Zhao et al., 1992), teleseismic receiver function (e.g., Ammon, 1991; Langston, 1979; Yuan et al., 1997),

and ambient noise tomography (e.g., Rawlinson et al., 2010). With such seismological tools in hand, large-scale, high-density seismic array data in East Asia have been used to image crustal and upper mantle structures with unprecedented detail. Improved imaging results with the retrieved three-dimensional velocity model provide additional constraints on defining tectonic boundaries, volcanism, crustal extensions, and lithospheric thinning that are currently in progress in northeastern China (e.g., Zheng et al., 2011). The seismic images can be additionally used to provide distinct interpretations of tectonic history. However, subsequent, quantitative geodynamic modeling is needed to better constrain past tectonic history.

4.1. Crustal properties of East Asia: Possible tectonic link between Korea and China

Since crustal composition is dissimilar from that of the mantle, the Moho provides evidence for the differentiation process of the Earth. Characteristics of the boundary between the crust and the uppermost mantle depend on the local geology and tectonic evolution of the area. In addition, crustal rock properties affected by the presence of fluids and/or changing crack geometry/distribution can be probed by measuring the ratio of compressional to shear wave velocity (V_p/V_s). Such crustal properties (crustal thickness and its V_p/V_s ratio) are typically obtained by stacking receiver functions (based on teleseismic P-to-S converted phase) for an individual station (Chen et al., 2010; Zhu and Kanamori, 2000; see Supplementary material for a short description on the method).

Crustal properties of the S. Korean Peninsula except the oceanic islands have been extensively studied by various seismological techniques such as receiver functions (Chang and Baag, 2007), joint inversion of surface wave dispersion and receiver functions (Chang and Baag, 2005; Yoo et al., 2007), waveform modeling (Kim et al., 2011), travel-time analysis (Jo and Hong, 2013), and refraction survey (Cho et al., 2006, 2013). The Moho beneath S. Korea is usually detected as a relatively well defined structure with lateral continuity (e.g., Chang and Baag, 2007). Most results show coherent and agreeable continental crust thickness (e.g., Fig. 3). Minor disagreements in values primarily come from the western and/or eastern coast of the Korean Peninsula and oceanic islands. This is mostly because of greater azimuthal variations in incoming seismic wave paths (e.g., continental versus oceanic paths). Only two recent studies (Yoo et al., 2007; Jo and Hong, 2013) report the crustal thickness of Jeju Island and the V_p/V_s of its upper crust, respectively. However, the resolution of the analyzed data might be poor due to insufficient station coverage on the island.

Excluding the results from the island, the crustal thickness of inland Korea varies from 25.9 km to 32.5 km, and the V_p/V_s from 1.71 to 1.82 (Fig. 3; Chang and Baag, 2007). The Korean Peninsula crust is slightly thinner than that of eastern China (31–35 km; Chen et al., 2010). Both crust-mantle interfaces appear to be relatively flat and sharp (i.e., large impedance contrast across the boundary). The V_p/V_s estimates by Chang and Baag (2007) clearly differ between different tectonic boundaries in S. Korea (Fig. 3), which might suggest different tectonic origin and/or history between the regions. At present, the continental crust of China is a mosaic of cratonic blocks and orogenic belts, which have diverse origins and experience complex histories of amalgamation (Santosh, 2010; Zheng et al., 2013, and references therein). By comparing their V_p/V_s estimates to those from a few stations in northeast China (Hetland et al., 2004), the most southern part of Korea (Yeongnam massif (YM); Fig. 3) might be closely related to the North China Craton in northeastern China (Chang and Baag, 2007). Because only few data are presented in Chang and Baag (2007), their argument needs to be verified by utilizing more recent and widely covered seismic data.

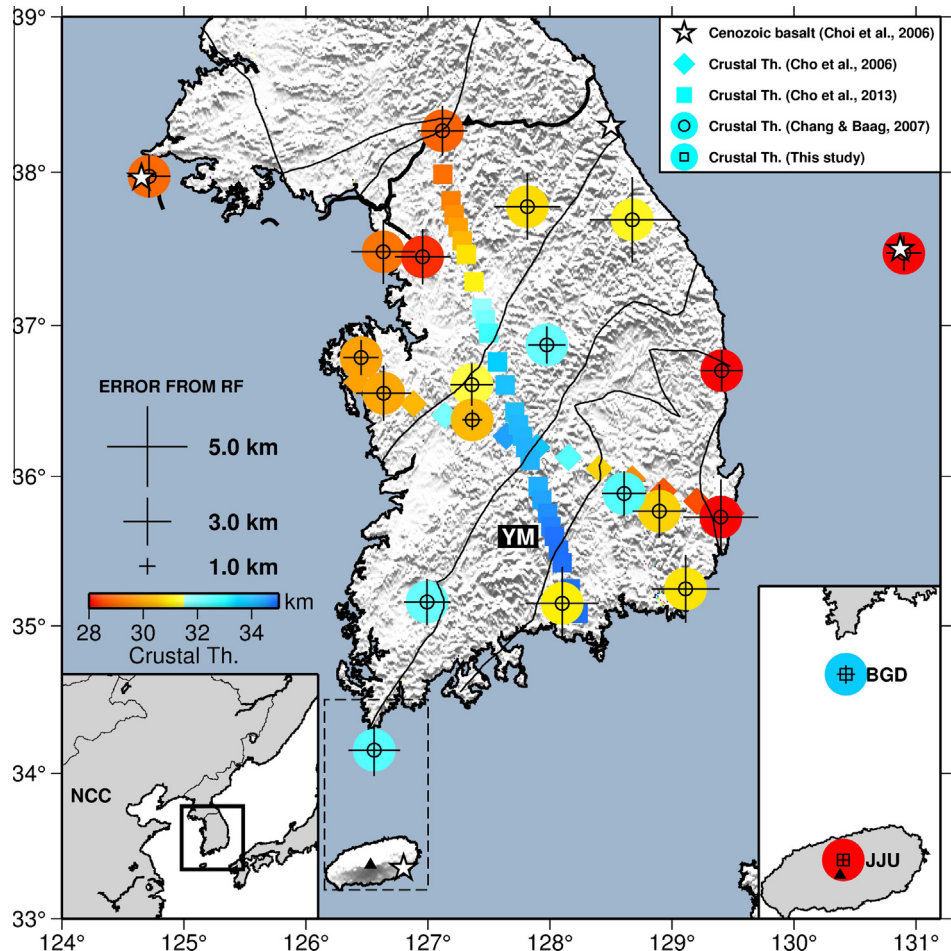


Fig. 3. Crustal thickness plotted on the topographic map of S. Korea. Lower-left inset illustrates the regional tectonic framework for East Asia. Three datasets independently constrained from seismic refractions KCRT2002 (Cho et al., 2006) and KCRT2004 (Cho et al., 2013), and teleseismic receiver functions (Chang and Baag, 2007) are shown in this figure. Error estimates of the crustal thickness derived from the receiver function (RF) analysis are also shown as crosses. In addition, geographical location of Cenozoic basaltic rock samples (Cho et al., 2006) is indicated as a star. Locations of volcanoes are shown as black triangles. Black thin lines delineate tectonic boundaries (Chough et al., 2000). Abbreviations shown in the figure are Yeongnam massif (YM) and North China Craton (NCC).

In addition, recent results from the ambient noise tomography based on Chinese and Japanese datasets (Zheng et al., 2011) show some shear speed variations among 0–80 km depth range beneath Korea, which are not fully discussed in the writings. Since Korean data is gathered only from a single station, we note that the resolution underneath Korea can be quite poor. Velocity transition (slow to fast from south to north, roughly) appears to occur near the southwestern margin of Korea (northwestern region of Jeju) at a depth of 60 km and beyond. In addition to this seismic observation, a clear gravity lineament trending northwest from Jeju Island to China (Shin et al., 2012) may indicate subsurface tectonic features, considering the bathymetry of the Yellow Sea is fairly flat.

4.2. Crustal properties of Jeju Island

As an example of the stacking method (Supplementary material), Fig. 4a and b shows the contour map of discontinuity depth and V_p/V_s ratio for stations BGD and JJU (locations shown in Fig. 3). Fig. 4c–d also shows receiver function seismograms and the resulting stack (last trace shown in blue¹). Table 1 summarizes crustal thickness, V_p/V_s , and Poisson's ratio for the two stations.

The Moho depth beneath Jeju Island is estimated to be 24.8 km (Fig. 4b), which is shallower than the nearby station BGD (33.6 km;

Fig. 4a) and the estimates for S. Korean crust (25.9–32.5 km; excluding results from Jeju Island) (Chang and Baag, 2007). Yoo et al. (2007) suggest that the crust of Jeju would be up to 35 km thick, based on joint inversion of receiver functions and surface-wave dispersion. This estimate is at least 10 km higher than that from the receiver functions. Average crustal V_p/V_s for Jeju Island is estimated to be 1.705 (Fig. 4b), which is smaller than the estimate from station BGD (1.77; Fig. 4a). Jo and Hong (2013) provide higher estimates (1.70–1.80) for the upper crust beneath the island.

Compared to the record section for BGD (Fig. 4c), the section for Jeju includes more complex signals after 3.5 s (Fig. 4d), clearly implying a different tectonic origin. Although the signal-to-noise ratio of seismograms recorded in Jeju Island appears low (compared to those from station BGD and other seismic stations), clear (positive) arrivals at ~2.9–3.5 s after P-wave arrival at 0.5 s for the Moho are observed (Fig. 4d). We have observed that waveforms of the arrival (at the base of the crust) look complicated (or distorted) in comparison to single, clean positive pulses at ~4.2 s obtained from station BGD (Fig. 4c). Such complex waveforms yield two peaks on the contour maps (Fig. 4b). This indicates either a gradual velocity increase for the Moho from ~20 km to 24.8 km depth or the presence of an additional thin (<5.0 km) layer just above the base of the crust.

Another seismological feature to note is consistently delayed P-arrivals at 0.5 s (Fig. 4d). Such delay in P is typically inferred to

¹ For interpretation of color in Fig. 4, the reader is referred to the web version of this article.

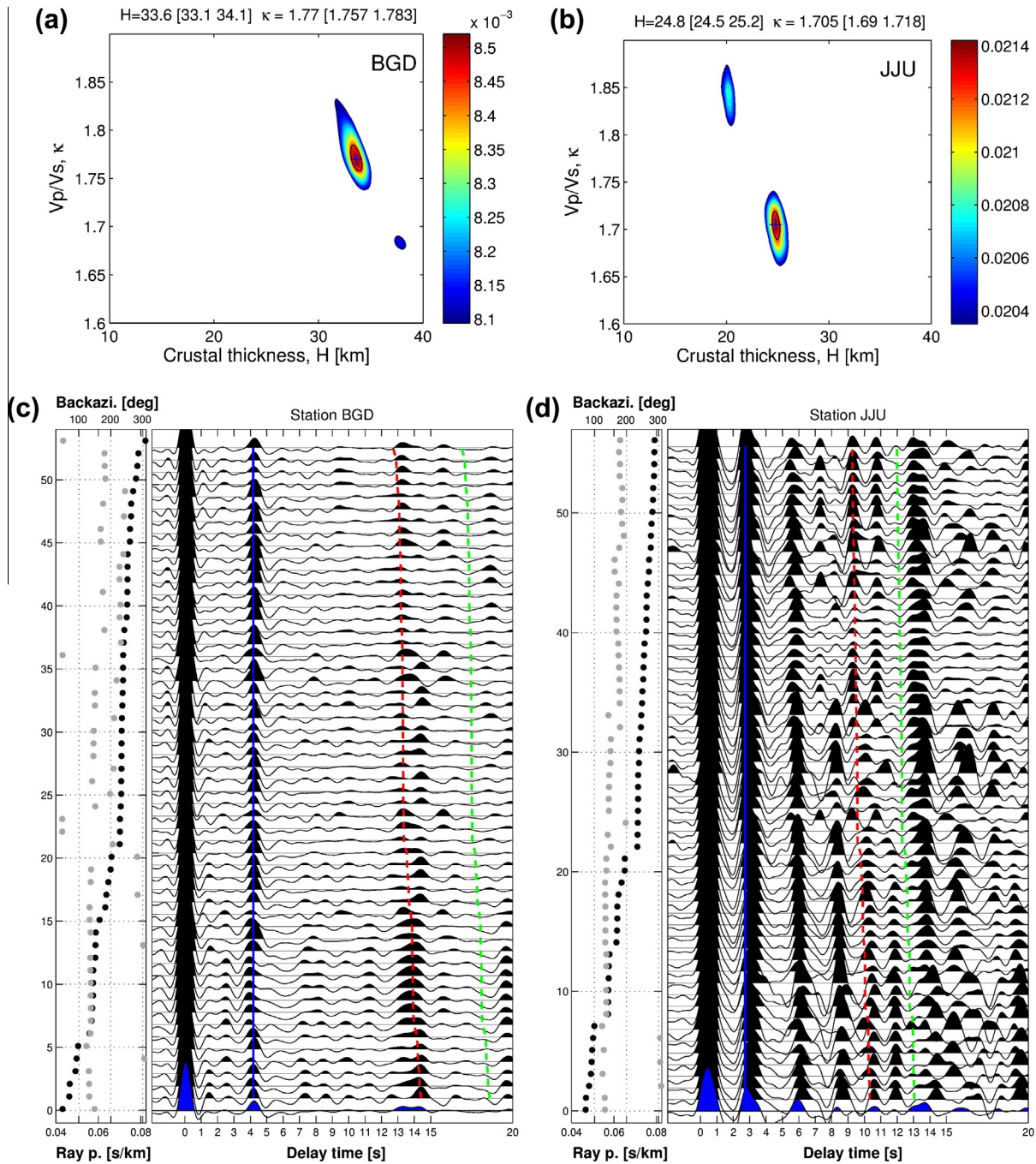


Fig. 4. Crustal thickness (Moho, discontinuity depth H) and P-to-S velocity ratio (Vp/Vs ratio, κ) for stations BGD and JJU. (a and b) Contour map of the weighted summation function (Zhu and Kanamori, 2000; Chen et al., 2010) for H and κ for stations BGD and JJU (station locations shown in the inset of Fig. 3). The black cross is the picked H and κ , which maximize the summation function. The black line is the 95% confidence bound, which represents their uncertainty estimate. Ranges in both H and κ within a 95% confidence bound are also specified at the top of the box. (c and d) Receiver functions sorted according to the ray parameter for stations BGD and JJU. Predicted arrival times of the primary phase (Pms; 'm' indicates a conversion at Moho) and two multiples (PpPms and PsPms) are marked by solid and dashed lines.

Table 1
Moho depth, P-to-S velocity ratio (Vp/Vs), and Poisson's ratio estimated for stations BGD (southern part of Korea; Fig. 3) and JJU (Jeju Island; Fig. 3), determined from receiver function analysis.

Station ID	Moho depth (km)	Vp/Vs	Poisson's ratio
BGD	33.6 ± 1.0	1.77 ± 0.026	0.266 ± 0.020
JJU	24.8 ± 0.7	1.705 ± 0.028	0.234 ± 0.026

be due to the near-surface structure. The time shift of 0.5 s may indicate the scattering induced by volcanic rocks present at a shallow depth (~ 4.0 km from the surface).

A series of negative and positive amplitude arrivals around $\sim 4\text{--}8$ s are clearly visible at all back azimuthal ranges (Fig. 4d), which can be used to predict additional layer(s) within the crust and/or at the uppermost mantle. The positive arrival at 6 s, if seismic multiple, require a velocity discontinuity within the crust ($\sim 15\text{--}17$ km). However, such positive arrival is absent in the section (Fig. 4d). Negative arrivals (at either 4–5 s or 7–8 s) after the positive conversion at the Moho may be an indication of the base of the lithosphere. This observation should be substantiated by another seismological tool (such as utilizing S-to-P phase). However, if true, we can assume that the lithospheric thickness is thin (<100 km)

beneath Jeju Island. Nevertheless, to be able to confirm this observation and be definitive on the interpretation, we need more seismic stations in Jeju to increase data coverage, and to model such complex, multiple phases to make sure that they are not reverberated phases from the near-surface structure.

Although the lithosphere–asthenosphere boundary (LAB) has important implications for mantle dynamics, the location is not well seismically imaged nor are its properties well understood. Furthermore, the effects of plume–lithosphere interaction on the depth of LAB are not well known. It has been hypothesized that the plume may locally decrease the lithospheric thickness (Li et al., 2004) or increase the thickness (Hall and Kincaid, 2003; Yamamoto and Morgan, 2009).

In an oceanic environment, decreases in velocity interpreted as the depth to the base of the lithosphere are observed at 40–140 km depth (Rychert et al., 2010). The global average from P-wave receiver functions for ocean island stations is 70 ± 4 km (Rychert and Shearer, 2009). However, these estimates do not necessarily represent a typical oceanic lithosphere, given that most of the locations are on top of a hot spot. Beneath Hawaii, the LAB deepens from 50 to 140 km from the oldest to the youngest, respectively (Collins et al., 2002; Li et al., 2000, 2004; Wolbern et al., 2006). The depths are estimated as 80 km beneath Iceland, 70 km and 100–120 km beneath eastern and western Greenland, respectively, and 40–60 km in Jan Mayan (Kumar et al., 2005) and the islands in the Indian Ocean (Kumar et al., 2007), respectively.

5. Numerical simulation for Cretaceous volcanism

Previously proposed plate reconstruction models cannot fully clarify two major geological episodes: generation and migration of adakites and A-type granitoids along the Japanese Islands, and intraplate magmatism in China. Partial melting of the relaminated cold plume and the lower mafic crust, magma mixing, and magma fractionalization would result in producing adakites (Castillo et al., 1999; Castro et al., 2013; Gerya and Yuen, 2003; Richards and Kerrich, 2007; Xu et al., 2002) in the Japanese Islands. However, these conditions cannot clearly explain adakites systematic southwest-to-northeast migration along the arc. In order to verify such constraints, numerical simulation is needed. Here we introduce two-dimensional numerical model experiments that consider the plume–slab interaction, which are similar to those in Lee and Lim (2014).

We artificially injected an anomalous heating source into the corner of the mantle wedge in order to trigger the partial melting of the subducted crust and to simulate the adakites along the Japanese Islands. To minimize computational costs, we have adopted a two-dimensional model framework, which can only cover southeastern Korea and Kyushu, Japan, where ages of the adakites and A-type granitoids are well constrained (Fig. 2a). Governing equations of the two-dimensional numerical kinematic-dynamic subduction models are based on an incompressible Boussinesq approximation (Kneller and van Keeken, 2008; Lee and King, 2010; Lee and Lim, 2014; Wada and Wang, 2009):

$$0 = \nabla \cdot \vec{v} \quad \text{continuity equation} \quad (1)$$

$$0 = -\nabla P + \nabla \cdot \bar{\tau} \quad \text{momentum equation} \quad (2)$$

$$\frac{DT}{Dt} = \nabla \cdot (k\nabla T) + H \quad \text{energy equation} \quad (3)$$

where \vec{v} is for velocity (m/s), P is for pressure (Pa), $\bar{\tau}$ is for deviatoric stress tensor (Pa), t is for time (s), and T is for temperature (°C). All

of the necessary parameters for the numerical experiments are summarized in Table 2.

We have fixed nodes for the thickness of the overriding crust at 35 km, which is similar to the estimate of current crustal thickness (Kamei, 2004), and assumes that its thickness is unaffected by underlying mantle behavior. To simulate the isolated serpentized corner of the mantle wedge (e.g., Currie et al., 2004), fixed nodes are extended to a depth of 50 km from the surface of the subducting slab. Since the dip of the subducting slab during the Cretaceous is not known, we used a ‘typical’ dip of 45° in our model experiments (e.g., Lee and King, 2009). A no-slip boundary condition is prescribed along the bottom of the overlying crust and mantle. A stress-free boundary condition is imposed to allow inflow/outflow of mantle behavior in the mantle wedge. An initial temperature profile is prescribed by using a half-space cooling model for a 50-Myr-old plate (mantle potential temperature of 1350 °C) and a mantle adiabat of 0.35 °C/km (1420 °C at a depth of 200 km). Radiogenic heat productions (Schubert et al., 2001) of 3.80×10^{-11} and 7.38×10^{-12} W/kg were used for the upper crust (thickness of 7 km), and the lower crust and underlying mantle, respectively.

The composite viscosity of diffusion and dislocation creep (Billen and Hirth, 2007; Karato and Wu, 1993) was used for dry olivine rheology of the mantle wedge:

$$\eta_{diff} = A_{diff}^{-1} d_g^m \exp \left[\frac{E_{diff} + PV_{diff}}{RT} \right] \quad \text{diffusion creep} \quad (4)$$

$$\eta_{disloc} = A_{disloc}^{-1/n} \times \exp \left[\frac{E_{disloc} + PV_{disloc}}{nRT} \right] \dot{\epsilon}_s^{1-n/n} \quad \text{dislocation creep} \quad (5)$$

$$\eta_{comp} = \left(\frac{1}{\eta_{diff}} + \frac{1}{\eta_{disloc}} \right)^{-1} \quad \text{composite viscosity} \quad (6)$$

The relevant notations and corresponding numerical values are described in Table 2. Considering the wet olivine rheology of the mantle wedge by fluids and volatiles from the dehydrating oceanic slab, viscosity reduction factor of 0.05 is multiplied to the calculated dry olivine rheology (e.g., Honda and Yoshida, 2005). Since the peak of the generation of adakites and A-type granitoids occur at ~105 Ma (Kinoshita, 1995, 2002), the peak of the temperature anomaly prescribed at the right wall of the mantle wedge is fixed at 110 Ma. The convergence rate and age of the subducting slab are approximated by using piecewise polynomials, and plate history is estimated from GPlates software (Gurnis et al., 2012; Williams et al., 2012). Additionally, we have exploited a trench-normal component in our model experiments considering that the behavior of the mantle wedge is mostly governed by the trench-normal component of the convergence velocity (Honda and Yoshida, 2005).

The lobe of the mantle plume, dragged into the corner of the mantle wedge, is assumed to reach the surface of the subducting slab. This results in triggering partial melting of the subducting slab, generating adakites and A-type granitoids in southern Korea and southwest Japan. To simulate the lobe of the mantle plume that has been dragged into the mantle wedge by the slab, we implemented a temporal temperature anomaly along the mantle wedge (right wall of the model domain) as a temporal temperature boundary condition (Fig. 5b). In this way, we can simulate the injection of the mantle plume into the mantle wedge without requiring large computational and technical costs (e.g., Lee and Lim, 2014). The temporal temperature boundary condition is implemented as a function of duration (σ_d) and thickness (σ_t) of the lobe of the mantle plume dragged to the mantle wedge and is expressed as a modified normal distribution function:

Table 2
Model input parameters.

<i>Model parameters</i>	
ρ , density (kg/m^3)	3300
T_{surf} , surface temperature ($^{\circ}\text{C}$)	0
ΔT , temperature contrast ($^{\circ}\text{C}$)	1420
C_p , heat capacity ($\text{J}/\text{kg K}$)	1200
k , thermal conductivity ($\text{W}/\text{m K}$)	3.96
H, radiogenic heat production (W/kg)	3.80×10^{-11} (upper crust) 7.38×10^{-12} (lower crust)
<i>Rheological parameters</i>	
E_{diff} (J/mol)	300×10^3
E_{disloc} (J/mol)	540×10^3
V_{diff} (m^3/mol)	6.0×10^{-6}
V_{disloc} (m^3/mol)	1.5×10^{-5}
A_{diff} ($\text{m}^{2.5}/\text{Pa s}$)	6.1×10^{-19}
A_{disloc} ($\text{s}^{1.5}/\text{Pa}^{3.5}$)	2.4×10^{-16}
d_g (m)	1.0×10^{-3}
m (-)	2.5
n (-)	3.5
R (J/mol)	8.314
<i>Plume parameters</i>	
T_a , temperature magnitude ($^{\circ}\text{C}$)	200
t_a , peak time (Ma)	110
σ_d , duration of the lobe injection (Myr)	2.5, 5.0, and 10.0
σ_a , thickness of the lobe injection (km)	20, 30, and 40
y_a , the core depth of the mantle plume (km)	100

E: activation energy, V: activation volume, A: prefactor, d_g : grain size, m: grain size exponent, n: stress exponent, and R: gas constant.

$$T_a * \exp \left\{ -\frac{(t - t_a)^2}{(\sigma_d)^2} \right\} * \exp \left\{ -\frac{(y - y_a)^2}{(\sigma_t)^2} \right\} \quad \text{temporal temperature anomaly} \quad (7)$$

The notations and corresponding numerical values related to the mantle plume are specified in Table 2. The peak temperature anomaly of the lobe is attained at 110 Ma (t_a). A temperature anomaly of 200 °C is used for T_a , yielding a peak lobe temperature of 1486.4 °C, which is a low end-member temperature of the mantle plume considering the cooling of the mantle plume lobe caused by ambient mantle. A depth of 100 km is used for y_a because the core of the mantle plume spreads laterally below the bottom of the lithosphere (Ribe and Christensen, 1994). Lobe durations of 2.5, 5.0, and 10 Myr and thicknesses of 20, 30, and 40 km are used independently in the simulation. These lobe durations and thicknesses are used to evaluate the thermal structure of the subducting slab.

The model domain of 200 km × 400 km (depth × width) is expressed as 200 × 400 four-node quadrilateral elements. A finite element code called 'ConMan' (King et al., 1990) is used to solve governing equations with mantle rheology and time-evolving subduction parameters. For the entire modeling run time, all trench-normal convergence rates, age of the slab, and temporal injection of the mantle plume are updated in each time step.

6. Numerical simulation results

Fig. 6 shows simulated temperature structures of the mantle wedge and the subducting slab at five different time slices, (a) 117.5, (b) 112.5, (c) 107.5, (e) 102.5 and (f) 97.5 Ma, at a duration of 10 Myr and a thickness of 30 km for the injected mantle plume. Fig. 6d shows the thermal structure at 107.5 Ma without the injection of mantle plume. Prior to the injection, anomalous temperature variations are not observed in the mantle wedge (Fig. 6a). However, as the lobe of the plume evolves in the back arc (at the right wall of the model domain), a hot mantle plume is dragged

into the corner of the wedge by corner flow. Subsequently, this induces an increase in slab temperature as the thermal boundary layer of the slab is thinned (Fig. 6b and c). The temperature of the mantle wedge without the presence of injected plume remains lower than the one with the plume (Fig. 6c vs. d). As the temperature anomaly in the back arc wanes over time, the vigor of the injected hot lobe consequently wanes, which results in a decreasing overall temperature at the mantle wedge and subducting slab (Fig. 6e). After 100 Ma, the effect of the temperature anomaly on the mantle wedge and subducting slab becomes negligible (Fig. 6f).

Fig. 7a–c shows a series of depth versus temperature curves of the subducting slab surface at 115, 110, 105, 100, and 95 Ma. Simulations are performed using a fixed thickness of the plume (30 km) and three different time durations (2.5, 5, and 10 Myr) of activity. Fig. 7d–f shows a series of slab surface temperature curves in time (Ma) at a slab depth of 100 km. Here, 100 km is considered as the deepest depth for the partial melting of the subducting slab, which is essential for generating adakites in the arc volcanoes (Mibe et al., 2011). Simulations are performed using three different lobe thickness values (20, 30, and 40 km), with a solidus of wet basalt (black dashed lines in Fig. 7d–f) (Kessel et al., 2005). If we use the low wet solidus of ~730° as suggested by Schmidt and Poli (1998), the partial melting of the subducted oceanic crust will be molten even in the absence of the plume lobe. This is not consistent with the presence of A-type granitoids and adakites in very short time duration. This issue can be resolved when we use a larger serpentinized corner of the mantle wedge by extending the vertical wall boundary to the slab surface at a depth of 70 km (e.g., Wada and Wang, 2009) instead of 50 km, which we used in this study. Accordingly, the dragged mantle flow into the corner of the mantle wedge is suppressed and the slab surface temperatures become lower than those of our model experiments.

The absence of mantle plume does not lead to slab melting due to a lower slab temperature (green dashed lines in Fig. 7), as also observed in a prior study (Lee and Ryu, 2016). However, if the mantle plume is dragged into the corner of the mantle wedge, as considered in this study, temporal plume–slab interaction occurs (Fig. 7a–c). For example, a numerical experiment using a duration of 5.0 Myr yields higher slab surface temperatures than the wet solidus of the oceanic crust at 110 and 105 Ma, implying a slab melting process (i.e., generation of adakites) in the arc (Fig. 7b). Temperature curves at 115 and 100 Ma only show marginal temperatures for the slab melting process, implying no or negligible adakites in the arc.

The evolution of slab surface temperature needs to be carefully examined during the experiment run because partial melting duration of the oceanic crust is crucial for the emplacement duration of adakites and A-type granitoids in the arc. Although debated, slab melts can reach the overlying lithosphere through the mantle wedge by diapirism or porous flow within a relatively short time (~1 Ma) (Gaetani and Grove, 2003; Grove et al., 2002). If correct, arc volcanism can be assumed to exist vertically above the slab surface where partial melting occurs. On this basis, we have traced a slab surface temperature at the depth of 100 km, considering the mean depth of the slab surface beneath the active volcanic front as ~100 km (Syracuse and Abers, 2006). The duration of the lobe of the mantle plume contributes linearly to the duration of pulse-like slab melting: 5, 10, and 20 Myr of slab melting for 2.5, 5, and 10 Myr lobe duration, respectively (Fig. 7d–f). We have not observed any notable effects induced by the lobe thickness on the duration of slab melting (Fig. 7d–f). Simulation results from the slab melting duration of 10 Myr can be well correlated with the generation duration (from ~120 to ~100 Ma) of adakites and A-type granitoids in southeast Korea and Kyushu (Fig. 7f). The slab

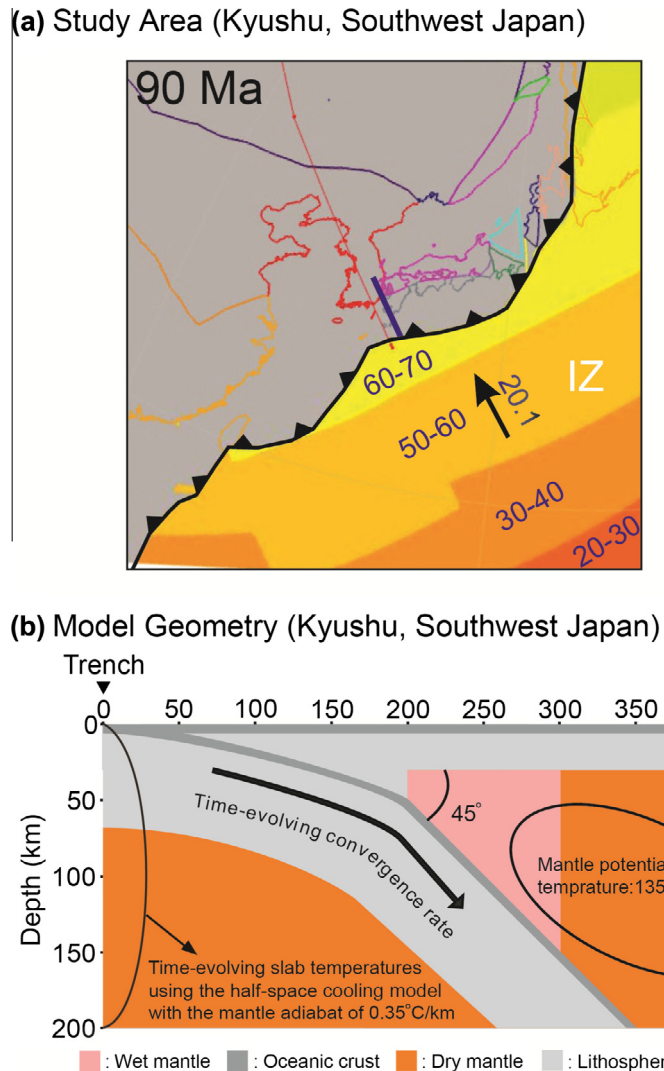


Fig. 5. The model set-up to examine the effect of mantle plume injection on the slab temperature. (a) The plate reconstruction model at 90 Ma. Thick blue line across southeastern Korea and Kyushu, Japan corresponds to the cross section of the modeled region shown in panel b. Before the opening of the East Sea (Sea of Japan; Fig. 1a), Korea and the Japanese Islands were joined together. Numbers on the Izanagi plate (IZ) indicate its plate age. The convergence rate of the IZ at 90 Ma is 20.1 cm/yr and the direction is shown as a black arrow. (b) Schematic diagram of the modeled region in the two-dimensional numerical model calculations. The subducting slab is kinematically imposed in the direction shown as a velocity vector (thick black arrow). The corner flow in the mantle wedge is induced by the subducting slab. Both convergence rate and slab age of the IZ are updated in each time step by using approximated piecewise polynomials of both parameters.

surface temperature curve does not show any slab melting feature without the presence of plume (green dashed line). Although our model calculations indicate that the duration of the injection of the plume lobe is ~ 10 Myr, the detailed duration and thickness of the plume lobe are worthy to evaluate in a time-evolving three-dimensional model. The temperature and/or flow structure of the plume lobe in the three-dimensional framework may be different than the trench-normal flow in the mantle wedge in the two-dimensional model framework.

7. Summary and synthesis

7.1. Proposed model for cretaceous volcanism in East Asia

The numerical calculation results (Fig. 7) strongly support the existence of intraplate mantle plume during the Cretaceous. We have successfully simulated the dragging of the plume lobe into the corner of the mantle wedge over the simulation run time, which correlates well with the partial melting process in the slab.

However, the southwest-to-northeast migration of adakites and A-type granitoids still remains unresolved. Such migration indicates that a heating source such as a hot lobe of the mantle plume should migrate along its same moving direction. The mantle plume has been usually considered as a fixed geological process for millions of years (e.g., Hawaii). Thus, it might be reasonable to assume that the mantle plume was fixed during the Cretaceous. If the plume is fixed geographically, the overlying plate should instead migrate to the opposite direction. Lee and Ryu (2016) suggest that the plate motion of the East Asian continental blocks show an average rate of 3.0 cm/yr from ca. 120 to 80 Ma, which is strikingly similar with the migration rate of the adakites and A-type granitoids along the Japanese Islands (Fig. 8).

Based on our simulation results, we argue that the intraplate magmatism in China can be related with mantle plume activity during the Cretaceous, either through large igneous province, radial dike swarm or swell, which are considered as typical expressions of plume activities, that have not been well constrained previously. However, recent numerical modeling studies indicate that so-called ‘typical’ expressions of the mantle plume may be

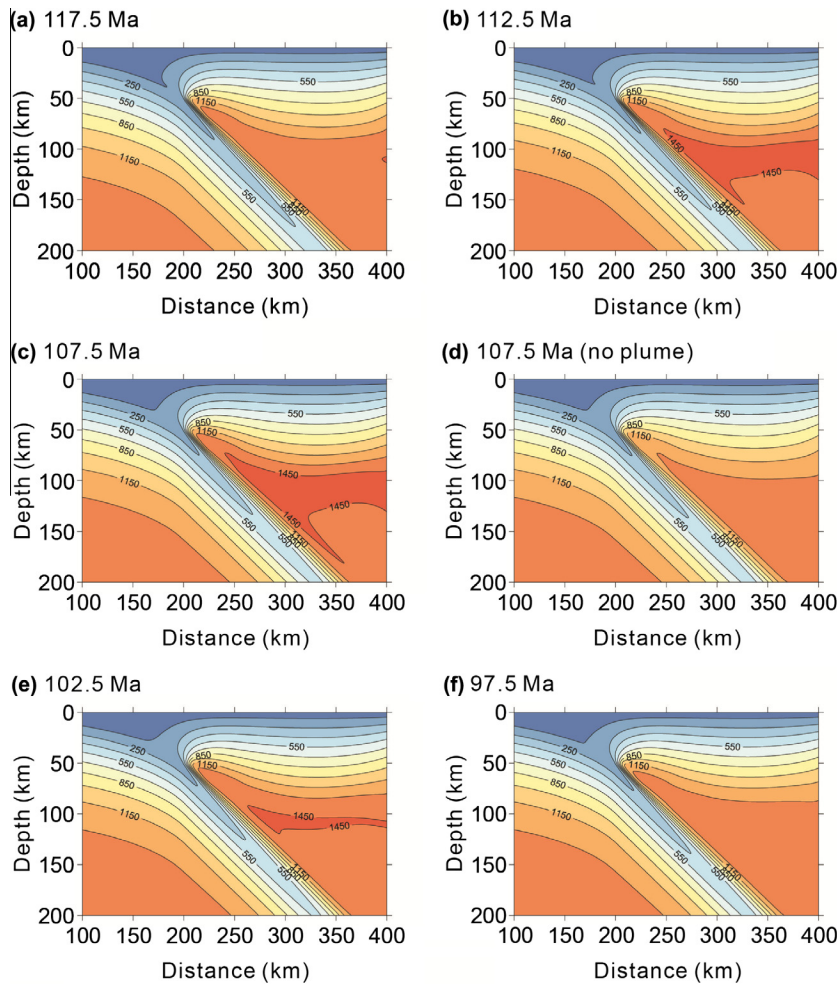


Fig. 6. Simulated thermal states for the mantle wedge and the subducting slab from the series of numerical experiments. Panels (a, b, c, e, and f) results based on the duration of 10 Myr and mantle plume lobe thickness of 30 km at 117.5, 112.5, 107.5, 102.5, and 97.5 Ma, respectively. Panel d shows experimental results excluding the lobe at 107.5 Ma. The unit of temperature is Celsius (°C), and the temperature contour is depicted every 150 °C. Horizontal distance indicates the distance from the trench.

irrelevant with the presence of the plume if it resides just beneath the continents (Ali et al., 2010; Betts et al., 2007; Burov et al., 2007). In addition, adakitic rocks and A-type granitoids can be associated with the mantle plume because they could be created by partial melting of delaminated lithosphere, and aided by excess heat of the underlying mantle plume. In particular, high Mg basalts such as picrites require very high mantle potential temperature, and cannot be easily correlated with the upwelling of mantle plume because adiabatic upwelling of the asthenosphere cannot generate excess heat energy used for generating high Mg basalts (Ernst and Buchan, 2003). Furthermore, basin-and-range type fault basins such as the Songliao and Bohaiwan basins can be considered as surficial expressions of the intraplate mantle plume (Burov et al., 2007). The massive intrusions of granitoids (130–110 Ma) in the Korean Peninsula resulting from the delamination of the overlying lithosphere (Kim et al., 2012) might be correlated to thermal erosion of the inflowing plume lobe beneath the lithosphere.

We suggest the following scenario to explain the Cretaceous volcanism in East Asia based on plume–slab interaction. An intraplate mantle plume in the early Cretaceous was established at ca. 140 Ma and has generated adakitic rocks and A-type granitoids through partial melting of the lower continental crust (Wang et al., 2006), picrites in western Shandong (~119 Ma) through the partial melting of hot asthenospheric mantle (Gao et al., 2008), and the Bohaiwan basin (from ~145 to ~130 Ma). As continental blocks migrate from northeast to southwest at a rate of

3.0 cm/yr (Gurnis et al., 2012; Sdrolias and Müller, 2006), intraplate adakitic rocks at ~125 Ma in Liaoning (Wu et al., 2005), A-type granitoids at ~125 Ma in Liaoning and Jilin (Wu et al., 2002, 2005), high Mg basalts at ~125 Ma in Liaoning (Gao et al., 2008), and Songliao basin from ~140 to ~110 Ma (Ren et al., 2002) may have formed during the migration. As the dragging of lobe of the intraplate mantle plume occurs, adakites and A-type granitoids are generated along the Japanese Islands.

7.2. Future perspectives: Proposal for the international ocean discovery program

Because both geophysical and geochemical data coverage is far from uniform across East Asia, there is still great difficulty relating compositional characteristics to geophysical properties (and vice versa). Consequently, various hypotheses have been put forward to explain the volcanism since Cretaceous. However, despite such difficulty, our numerical simulation results have opened a new and interesting discussion on the origin of the Cretaceous intraplate volcanism in the vicinity of China, Korea and Japan and back-arc opening in a wider context of global geodynamics. To verify and/or efficiently constrain our model for the plume–slab interaction, we suggest the following proposals.

Accurate and detailed mapping of volcanic rocks is the most critical step for all subsequent investigations. Detailed geochronological investigations on volcanic history of individual volcanic

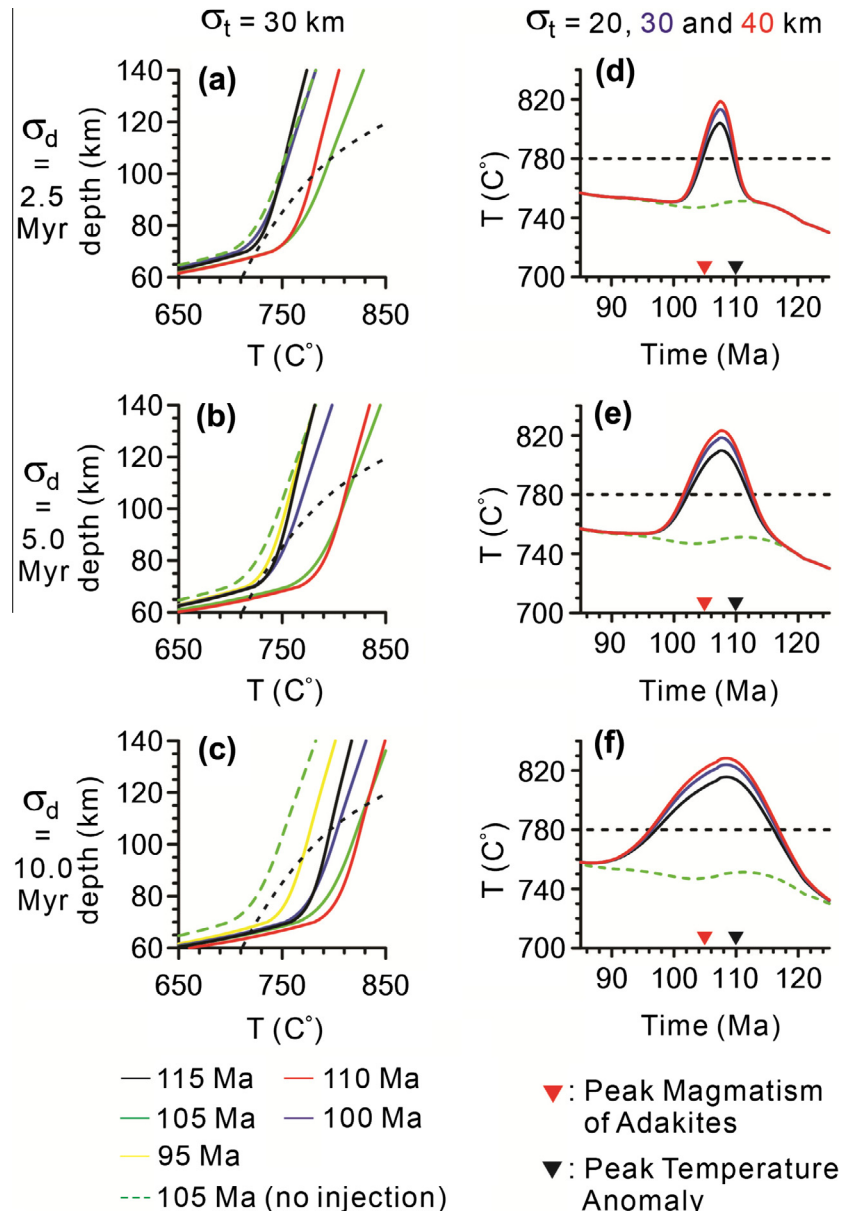


Fig. 7. Numerical simulation results. (a–c) Depth versus temperature of the subducting slab depicted every 5 Myr from 115 to 95 Ma for durations of 2.5, 5.0, and 10 Myr and 30 km thickness of the dragged lobe of the mantle plume. (d–f) Temporal evolution of the slab surface temperature from 125 Ma to 85 Ma at a depth of 100 km. The 100 km depth is a reasonable depth for generating adakites, showing the partial melting of the subducting slab. Black, blue, and red colored curves correspond to the vertical thickness of the lobe of the mantle plume as 20, 30, and 40 km, respectively. The green dashed line represents no partial melting of the subducting oceanic crust at ~105 Ma and peak adakite magmatism in southwestern Korea and Kyushu, Japan. (For interpretation of the references to color in this figure legend, the reader is referred to the web version of this article.)

fields based on mapping are necessary to reveal the spatial-time evolution of volcanic activities. Currently, there is a data gap between southern China and the region near Jeju Island (southwestern margin of Korea) (e.g., Choi et al., 2006), which can be filled by acquiring a direct sample of the oceanic crust. This is the region where high gravity anomaly values (Fig. 1b; Shin et al., 2012) and lower shear wave velocities at the uppermost mantle depth (Zheng et al., 2011) are observed. Geophysical evidence may indicate the presence of buried intrusive and/or volcanic features. In addition, a clear gravity lineament trending northwest from Jeju Island to China (Shin et al., 2012) may reveal subsurface tectonic features. A detailed geophysical survey is necessary to clarify the origin of such gravity lineament and lower shear speeds and their implication to the tectonics of East Asia.

This drilling site may provide a pathway to unravel the origin of the volcanic oceanic islands around Korea and a possible link to the tectonics of the region of China.

Sedimentary, petrologic, and in-situ borehole geophysical data from the proposed drilling site can be used to assess various hypotheses on the origin of Cenozoic intraplate volcanism, particularly for Jeju Island. In particular, sedimentary facies can provide subsidence and uplift history of the island after its emplacement. In-situ borehole geophysical data can show the status of stress caused by the current tectonic setting as well as its temporal variation.

Finally, based on our numerical results, we presume that adakites and A-type granitoids are emplaced along the ancient subduction zone margin in East Asia (southeastern China, southwest

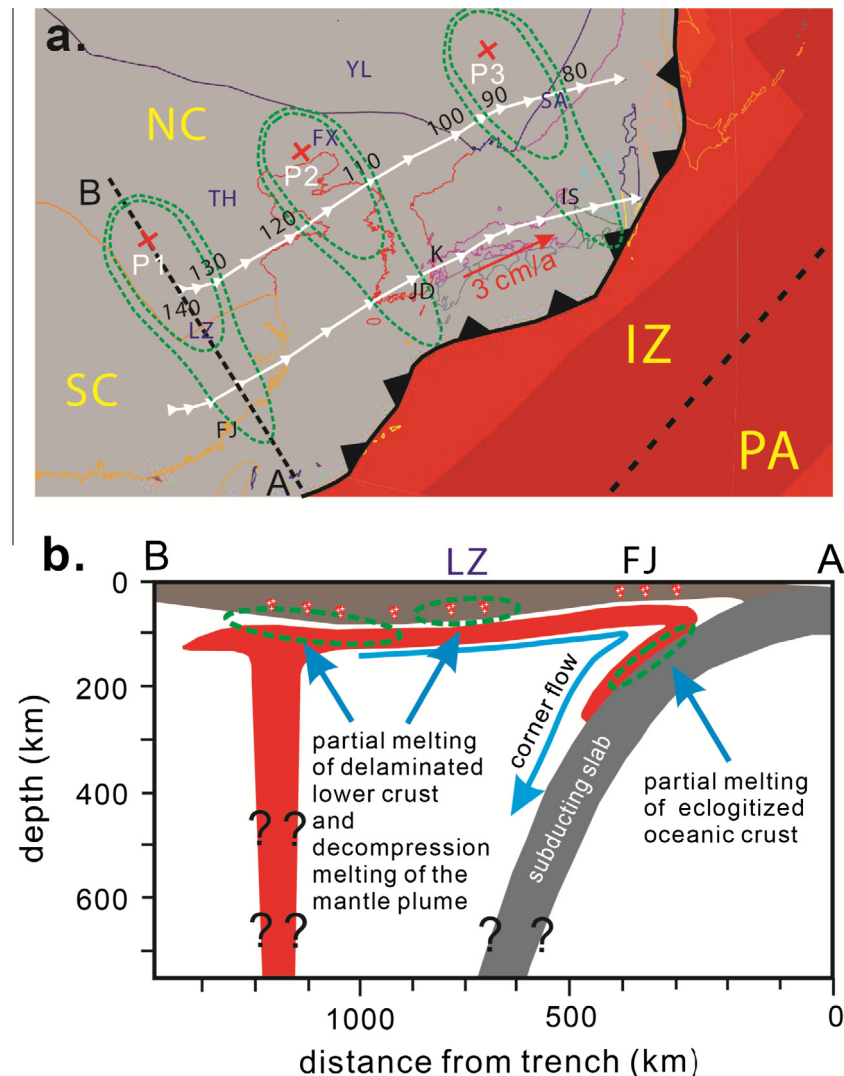


Fig. 8. Schematic diagram showing the apparent migration of the intraplate mantle plume across the East Asian region during the Cretaceous (a), and the cross section of the intraplate mantle plume and the interaction between dragged lobe of the mantle plume and subducting slab at ca. 125 Ma (b) (modified from Lee and Ryu, 2016). (a) Although the mantle plume has been regarded as fixed during the Cretaceous, the northeast-to-southwest migration of the East Asian region resulted in the opposite direction of the apparent migration of the mantle plume, which had proceeded from southwest to northeast. Numbers shown along the white color trajectory indicates the estimated ages (Ma). By GPlates software (Gurnis et al., 2012; Williams et al., 2012), the migration rate of the East Asian region has been estimated as 3 cm/yr, which is strikingly consistent with the migration rate of adakites and A-type granitoids along the Japanese arc. (b) Cross section along the dashed line in a. The section shows a rising mantle plume and the lobe of the mantle plume dragged to the corner of the mantle wedge, resulting in partial melting of the subducted oceanic crust.

Yellow Sea and the Japanese Islands). The presence of adakites and A-type granitoids in the southwest Yellow Sea via oceanic drilling clearly support our model of Cretaceous volcanism and suggest a revised view on the diverse interactions between the intraplate mantle plume and continental/oceanic plates.

Acknowledgements

This study was a part of the K-IODP project through Korea Institute of Geoscience and Mineral Resources funded by the Ministry of Oceans and Fisheries, Korea. Y. Kim was supported by the Aspiring Researcher Program through Seoul National University in 2014, and National Research Foundation (NRF) of Korea Grant funded by the Korean Government (NRF-2014S1A2A2027609). C. Lee was supported by the NRF of Korea Grant funded by the Ministry of Education, Science and Technology of Korean Government (NRF-35B-2011-1-C00043). S. Kim acknowledges support from the Basic Science Research

Program through NRF (NRF-2013R1A1A1076071) funded by the Ministry of Science, ICT & Future Planning, Korea. Finally, the authors thank the special issue guest editor Sanghoon Kwon and two anonymous reviewers for helpful comments, which greatly improved the paper.

Appendix A. Supplementary material

Supplementary data associated with this article can be found, in the online version, at <http://dx.doi.org/10.1016/j.jseaes.2015.07.032>.

References

- Ali, J.R., Fitton, J.G., Herzberg, C., 2010. Emeishan large igneous province (SW China) and the mantle-plume up-doming hypothesis. *J. Geol. Soc.* 167 (5), 953–959.
- Ammon, C.J., 1991. The isolation of receiver effects from teleseismic P waveforms. *Bull. Seismol. Soc. Am.* 81, 2504–2510.
- Basu, A.R., Wang, J.W., Huang, W.K., Xie, G.H., Tatsumoto, M., 1991. Major element, REE, and Pb, Nd and Sr isotopic geochemistry of Cenozoic volcanic rocks of

- eastern China: implications for their origin from suboceanic-type mantle reservoirs. *Earth Planet. Sci. Lett.* 105, 149–169.
- Betts, P.G., Giles, D., Schaefer, B.F., Mark, G., 2007. 1600–1500 Ma hotspot track in eastern Australia: implications for Mesoproterozoic continental reconstructions. *Terra Nova* 19 (6), 496–501.
- Bijwaard, H., Spakman, W., Engdahl, E.R., 1998. Closing the gap between regional and global travel time tomography. *J. Geophys. Res.* 103, 30055–30078.
- Billen, M.I., Hirth, G., 2007. Rheologic controls on slab dynamics. *Geochem. Geophys. Geosyst.* 8 (8), Q08012.
- Burov, E., Guillou-Frottier, L., d'Arcemont, E., Le Pourhiet, L., Cloetingh, S., 2007. Plume head–lithosphere interactions near intra-continental plate boundaries. *Tectonophysics* 434 (1–4), 15–38.
- Castillo, P.R., Janney, P.E., Solidum, R.U., 1999. Petrology and geochemistry of Camiguin Island, southern Philippines: insights to the source of adakites and other lavas in a complex arc setting. *Contrib. Miner. Petrol.* 134 (1), 33–51.
- Castillo, P.R., 2012. Adakite petrogenesis. *Lithos* 134–135, 304–316.
- Castro, A., Vogt, K., Gerya, T., 2013. Generation of new continental crust by sublithospheric silicic-magma relamination in arcs: a test of Taylor's andesite model. *Gondwana Res.* 23 (4), 1554–1566.
- Chang, S.-J., Baag, C.-E., 2005. Crustal structure in southern Korea from joint analysis of teleseismic receiver functions and surface-wave dispersion. *Bull. Seismol. Soc. Am.* 95 (4), 1516–1534. <http://dx.doi.org/10.1785/0120040080>.
- Chang, S.-J., Baag, C.-E., 2007. Moho depth and crustal V_p/V_s variation in southern Korea from teleseismic receiver functions: implication for tectonic affinity between the Korean Peninsula and China. *Bull. Seismol. Soc. Am.* 97 (5), 1621–1631. <http://dx.doi.org/10.1785/0120050264>.
- Chen, Y., Zhang, Y., Graham, D., Su, S., Deng, J., 2007. Geochemistry of Cenozoic basalts and mantle xenoliths in Northeast China. *Lithos* 96 (1–2), 108–126.
- Chen, Y., Niu, F., Liu, R., Huang, Z., Tkalcic, H., Sun, L., Chan, W., 2010. Crustal structure beneath China from receiver function analysis. *J. Geophys. Res.* 115 (B03307). <http://dx.doi.org/10.1029/2009JB006386>.
- Cho, H.-M., Baag, C.-E., Lee, J.M., Moon, W.M., Jung, H., Kim, K.Y., Asudeh, I., 2006. Crustal velocity structure across the southern Korean Peninsula from seismic refraction survey. *Geophys. Res. Lett.* 33 (L06307). <http://dx.doi.org/10.1029/2005GL025145>.
- Cho, H.-M., Baag, C.-E., Lee, J.M., Moon, W.M., Jung, H., Kim, K.Y., 2013. P- and S-wave velocity model along crustal scale refraction and wide-angle reflection profile in the southern Korean Peninsula. *Tectonophysics* 582, 84–100. <http://dx.doi.org/10.1016/j.tecto.2012.09.025>.
- Choi, S.H., Mukasa, S.B., Kwon, S.-T., Andronikov, A.V., 2006. Sr, Nd, Pb and Hf isotopic compositions of late Cenozoic alkali basalts in South Korea: evidence for mixing between the two dominant asthenospheric mantle domains beneath East Asia. *Chem. Geol.* 232 (3–4), 134–151.
- Chough, S.K., Kwon, S.-T., Ree, J.-H., Choi, D.K., 2000. Tectonic and sedimentary evolution of the Korean peninsula: a review and new view. *Earth Sci. Rev.* 52, 175–235.
- Collins, J.A., Vernon, F.L., Orcutt, J.A., Stephen, R.A., 2002. Upper mantle structure beneath the Hawaiian swell: constraints from the ocean seismic network pilot experiment. *Geophys. Res. Lett.* 29 (11), 1522. <http://dx.doi.org/10.1029/2001GL013302>.
- Currie, C.A., Wang, K., Hyndman, R.D., He, J., 2004. The thermal effects of steady-state slab-driven mantle flow above a subducting plate: the Cascadia subduction zone and backarc. *Earth Planet. Sci. Lett.* 223 (1–2), 35–48.
- Dyksterhuis, S., Müller, R.D., Albert, R.A., 2005. Paleostress field evolution of the Australian continent since the Eocene. *J. Geophys. Res.* 110 (B05102). <http://dx.doi.org/10.1029/2003JB002728>.
- Dyksterhuis, S., Müller, R.D., 2008. Cause and evolution of intraplate orogeny in Australia. *Geology* 36, 495–498. <http://dx.doi.org/10.1130/G24536A.1>.
- Ernst, R.E., Buchan, K.L., 2003. Recognizing mantle plumes in the geological record. *Annu. Rev. Earth Planet. Sci.* 31, 469–523.
- Fukao, Y., Obayashi, M., Nakakuki, T., The Deep Slab Project Group, 2009. Stagnant slab: a review. *Annu. Rev. Earth Planet. Sci.* 37, 19–46. <http://dx.doi.org/10.1146/annurev.earth.36.031207.124224>.
- Gaetani, G.A., Grove, T.L., 2003. Experimental constraints on melt generation in the mantle wedge: in inside the subduction factory. *Geophys. Monogr. Ser.* 138, 107–134.
- Gaina, C., Müller, D., 2007. Cenozoic tectonic and depth/age evolution of the Indonesian gateway and associated back-arc basins. *Earth Sci. Rev.* 83 (3–4), 177–203.
- Gao, S., Rudnick, R.L., Xu, W.-L., Yuan, H.-L., Liu, Y.-S., Walker, R.J., Puchtel, I.S., Liu, X., Huang, H., Wang, X.-R., Yang, J., 2008. Recycling deep cratonic lithosphere and generation of intraplate magmatism in the North China Craton. *Earth Planet. Sci. Lett.* 270 (1–2), 41–53.
- Gerya, T.V., Yuen, D.A., 2003. Rayleigh–Taylor instabilities from hydration and melting propel ‘cold plumes’ at subduction zones. *Earth Planet. Sci. Lett.* 212 (1–2), 47–62.
- Gibbons, A., Zahirovic, S., Müller, R.D., Whittaker, J., Yatheesh, V., 2015. A tectonic model reconciling evidence for the collision between India, Eurasia and intra-oceanic arcs of the central-eastern Tethys. *Gondwana Res.* <http://dx.doi.org/10.1016/j.gr.2015.01.001> (in press).
- Grove, T., Parman, S., Bowring, S., Price, R., Baker, M., 2002. The role of an H_2O -rich fluid component in the generation of primitive basaltic andesites and andesites from the Mt. Shasta region, N California. *Contrib. Miner. Petrol.* 142 (4), 375–396.
- Gurnis, M., Turner, M., Zahirovic, S., DiCaprio, L., Spasojevic, S., Müller, R.D., Boyden, J., Seton, M., Manea, V.C., Bower, D.J., 2012. Plate tectonic reconstructions with continuously closing plates. *Comput. Geosci.* 38 (1), 35–42.
- Hall, P.S., Kincaid, C., 2003. Melting, dehydration, and the dynamics of off-axis plume-ridge interaction. *Geochem. Geophys. Geosyst.* 4 (9), 8510. <http://dx.doi.org/10.1029/2003GC000567>.
- Heidbach, O., Tingay, M., Barth, A., 2008. Reinecker, J., Kurfeß, D., Müller, B., 2008. The World Stress Map Database Release. <http://dx.doi.org/10.1594/GFZ.WSM.Rel2008>.
- Heine, C., Müller, D., Gaina, C., 2004. Reconstructing the Lost Eastern Tethys Ocean Basin: Convergence history of the SE Asian margin and marine gateways. In: Clift, P. et al. (Ed.), *Continent-Ocean Interactions in Southeast Asia*. American Geophysical Monograph, vol. 149, Washington, pp. 37–54.
- Hetland, E.A., Wu, F.T., Song, J.L., 2004. Crustal structure in the Changbaishan volcanic area, China, determined by modeling receiver functions. *Tectonophysics* 386, 157–175.
- Honda, S., Yoshida, T., 2005. Effects of oblique subduction on the 3-D pattern of small-scale convection within the mantle wedge. *Geophys. Res. Lett.* 32 (13), L13307.
- Huang, J., Zhao, D., 2006. High-resolution mantle tomography of China and surrounding regions. *J. Geophys. Res.* 111 (B09305). <http://dx.doi.org/10.1029/2005JB004066>.
- Huang, Z., Zhao, D., Hasagawa, A., Umino, N., Park, J.-H., Kang, I.-B., 2013. Aseismic deep subduction of the Philippine Sea plate and slab window. *J. Asian Earth Sci.* 75, 82–94. <http://dx.doi.org/10.1016/j.jseas.2013.07.002>.
- Isozaki, Y., Aoki, K., Nakama, T., Yanai, S., 2010. New insight into a subduction-related orogen: A reappraisal of the geotectonic framework and evolution of the Japanese Islands. *Gondwana Res.* 18 (1), 82–105.
- Jo, E., Hong, T.-K., 2013. V_p/V_s ratios in the upper crust of the southern Korean Peninsula and their correlations with seismic and geophysical properties. *J. Asian Earth Sci.* 66, 204–214.
- Kamei, A., 2004. An adakitic pluton on Kyushu Island, southwest Japan arc. *J. Asian Earth Sci.* 24 (1), 43–58.
- Karato, S.-I., Wu, P., 1993. Rheology of the upper mantle: a synthesis. *Science* 260, 771–778.
- Kessel, R., Ulmer, P., Pettke, T., Schmidt, M.W., Thompson, A.B., 2005. The water-basalt system at 4 to 6 GPa: phase relations and second critical endpoint in a K -free eclogite at 700 to 1400 °C. *Earth Planet. Sci. Lett.* 237 (3–4), 873–892.
- Kim, S., Rhie, J., Kim, G., 2011. Forward waveform modeling procedure for 1-D crustal velocity structure and its application to the southern Korean Peninsula. *Geophys. J. Int.* 185, 453–468. <http://dx.doi.org/10.1111/j.1365-246X.2011.04949.x>.
- Kim, S.W., Kwon, S., Ryu, I.-C., Jeong, Y.-J., Choi, S.-J., Kee, W.-S., Yi, K., Lee, Y.S., Kim, B.C., Park, D.W., 2012. Characteristics of the early Cretaceous igneous activity in the Korean Peninsula and tectonic implications. *J. Geol.* 120, 625–646.
- King, S.D., Raefsky, A., Hager, B.H., 1990. Conman: vectorizing a finite element code for incompressible two-dimensional convection in the Earth's mantle. *Phys. Earth Planet. Inter.* 59 (3), 195–207.
- Kinoshita, O., 1995. Migration of igneous activities related to ridge subduction in Southwest Japan and the East Asian continental margin from the Mesozoic to the Paleogene. *Tectonophysics* 245 (1–2), 25–35.
- Kinoshita, O., 2002. Possible manifestations of slab window magmatism in Cretaceous southwest Japan. *Tectonophysics* 344 (1–2), 1–13.
- Kneller, E.A., van Keeken, P.E., 2008. Effect of three-dimensional slab geometry on deformation in the mantle wedge: implications for shear wave anisotropy. *Geochem. Geophys. Geosyst.* 9 (1), Q01003.
- Kumar, P., Kind, R., Hanka, W., Wylegalla, K., Reigber, C., Yuan, X., Woelbern, I., Schwintzer, P., Fleming, K., Dahl-Jensen, T., Larsen, T.B., Schweitzer, J., Priestley, K., Gudmundsson, O., Wolf, D., 2005. The lithosphere–asthenosphere boundary in the North-West Atlantic region. *Earth Planet. Sci. Lett.* 236 (1–2), 249–257.
- Kumar, P., Yuan, X., Kumar, M.R., Kind, R., Li, X., Chadha, R.K., 2007. The rapid drift of the Indian tectonic plate. *Nature* 449 (7164), 894–897.
- Kuritani, T., Ohtani, E., Kimura, J.-I., 2011. Intensive hydration of the mantle transition zone beneath China caused by ancient slab stagnation. *Nat. Geosci.* 4, 713–716. <http://dx.doi.org/10.1038/NGEO1250>.
- Langston, C.A., 1979. Structure under Mount Rainier, Washington, inferred from teleseismic body waves. *J. Geophys. Res.* 84 (B9), 4749–4762. <http://dx.doi.org/10.1029/JB084iB09p04749>.
- Lee, C., King, S.D., 2009. Effect of mantle compressibility on the thermal and flow structures of the subduction zones. *Geochem. Geophys. Geosyst.* 10 (1), Q01006.
- Lee, C., King, S.D., 2010. Why are high-Mg# andesites widespread in the western Aleutians? A numerical model approach. *Geology* 38 (7), 583–586.
- Lee, C., Lim, C., 2014. Short-term and localized plume–slab interaction explains the genesis of Abukuma adakite in Northeastern Japan. *Earth Planet. Sci. Lett.* 396, 116–124.
- Lee, C., Ryu, I.-C., 2016. A new tectonic model for the genesis of adakitic arc magmatism in Cretaceous East Asia. In: Morra, G., Yuen, D.A., King, S.D., Lee, S.-M. (Eds.), *Subduction Dynamics: From Mantle Flow to Mega Disasters*. John Wiley & Sons Inc, Hoboken, NJ, pp. 69–79 (in press).
- Li, X., Kind, R., Priestley, K., Sobolev, S.V., Tilman, F., Yuan, X., Weber, M., 2000. Mapping the Hawaiian plume conduit with converted seismic waves. *Nature* 405 (6789), 938–941.
- Li, X., Kind, R., Yuan, X.H., Wolbern, I., Hanka, W., 2004. Rejuvenation of the lithosphere by the Hawaiian plume. *Nature* 427 (6977), 827–829.
- Li, C., van der Hilst, R.D., Engdahl, E.R., Burdick, S., 2008. A new global model for P wave speed variations in Earth's mantle. *Geochem. Geophys. Geosyst.* 9 (5), 1–21.
- Liu, M., Yang, Y., Shen, Z., Wang, S., Wang, M., Wan, Y., 2007. Active tectonics and intracontinental earthquakes in China: the kinematics and geodynamics. *Geol. Soc. Am. Spec. Pap.* 425, 299–318. [http://dx.doi.org/10.1130/2007.2425\(19\)](http://dx.doi.org/10.1130/2007.2425(19)).

- Long, M.D., Hager, B.H., de Hoop, M.V., van der Hilst, R.D., 2007. Two-dimensional modelling of subduction zone anisotropy with application to southwestern Japan. *Geophys. J. Int.* 170, 839–856.
- Maruyama, S., Isozaki, Y., Kimura, G., Terabayashi, M., 1997. Paleogeographic maps of the Japanese Islands: plate tectonic synthesis from 750 Ma to the present. *Isl. Arc* 6 (1), 121–142.
- Menzies, M., Xu, Y., Zhang, H., Fan, W., 2007. Integration of geology, geophysics and geochemistry: a key to understanding the North China Craton. *Lithos* 96 (1–2), 1–21.
- Mibe, K., Kawamoto, T., Matsukage, K.N., Fei, Y., Ono, S., 2011. Slab melting versus slab dehydration in subduction-zone magmatism. *Proc. Natl. Acad. Sci. USA* 108, 8177–8182. <http://dx.doi.org/10.1073/pnas.1010968108>.
- Müller, R.D., Sdrolias, M., Gaina, C., Steinberger, B., Heine, C., 2008. Long-term sea-level fluctuations driven by ocean basin dynamics. *Science* 319 (5868), 1357–1362.
- Nakamura, E., Campbell, I.H., McCulloch, M.T., Sun, S.-S., 1989. Chemical geodynamics in a back arc region around the Sea of Japan: implications for the genesis of alkaline basalts in Japan, Korea, and China. *J. Geophys. Res.* 94 (B4), 4634.
- Okada, H., 1999. Plume-related sedimentary basins in East Asia during the Cretaceous. *Palaeogeogr. Palaeoclimatol. Palaeoecol.* 150 (1–2), 1–11.
- Peng, Z.C., Zartman, R.E., Futa, K., Chen, D.G., 1986. Pb-, Sr- and Nd-isotopic systematics and chemical characteristics of Cenozoic basalts, Eastern China. *Chem. Geol.* 59, 3–33.
- Rawlinson, N., Pozgay, S., Fishwick, S., 2010. Seismic tomography: a window into deep Earth. *Phys. Earth Planet. Inter.* 178, 101–135. <http://dx.doi.org/10.1016/j.pepi.2009.10.002>.
- Ren, J., Tamaki, K., Li, S., Junxia, Z., 2002. Late Mesozoic and Cenozoic rifting and its dynamic setting in Eastern China and adjacent areas. *Tectonophysics* 344 (3–4), 175–205.
- Ribe, N.M., Christensen, U.R., 1994. 3-Dimensional modeling of plume–lithosphere interaction. *J. Geophys. Res.* 99 (B1), 669–682.
- Richards, J.P., Kerrich, R., 2007. Special paper: adakite-like rocks: their diverse origins and questionable role in metallogenesis. *Econ. Geol.* 102 (4), 537–576.
- Rychert, C.A., Shearer, P.M., 2009. A global view of the lithosphere–asthenosphere boundary. *Science* 324 (5926), 495–498.
- Rychert, C.A., Shearer, P.M., Fischer, K.M., 2010. Scattered wave imaging of the lithosphere–asthenosphere boundary. *Lithos* 173–185. <http://dx.doi.org/10.1016/j.lithos.2009.12.006>.
- Sandwell, D.T., Smith, W.H.F., 2009. Global marine gravity from retracked Geosat and ERS-1 altimetry: ridge segmentation versus spreading rate. *J. Geophys. Res.* 114 (B01411). <http://dx.doi.org/10.1029/2008JB006008>.
- Sandwell, D.T., Garcia, E., Soofi, K., Wessel, P., Smith, W.H.F., 2013. Towards 1 mGal global marine gravity from CryoSat-2, Envisat, and Jason-1. *Lead. Edge* 32 (8), 892–899. <http://dx.doi.org/10.1190/tle32080892.1>.
- Sandwell, D.T., Müller, R.D., Smith, W.H.F., Garcia, E., Francis, R., 2014. New global marine gravity model from CryoSat-2 and Jason-1 reveals buried tectonic structure. *Science* 346 (6205), 65–67. <http://dx.doi.org/10.1126/science.1258213>.
- Santosh, M., 2010. Assembling North China Craton within the Columbia supercontinent: the role of double-sided subduction. *Precambr. Res.* 178, 149–167. <http://dx.doi.org/10.1016/j.precamres.2010.02.003>.
- Schmidt, M.W., Poli, S., 1998. Experimentally based water budgets for dehydrating slabs and consequences for arc magma generation. *Earth Planet. Sci. Lett.* 163 (1–4), 361–379.
- Schubert, G., Turcotte, D.L., Olson, P., 2001. *Mantle Convection in the Earth and Planets*. Cambridge University Press.
- Sdrolias, M., Müller, R.D., 2006. Controls on back-arc basin formation. *Geochem. Geophys. Geosyst.* 7 (Q04016). <http://dx.doi.org/10.1029/2005GC001090>.
- Shin, Y.H., Choi, K.S., Koh, J.-S., Yun, S.-H., Nakamura, E., Na, S.-H., 2012. Lithospheric-folding-based understanding on the origin of the back-arc basaltic magmatism beneath Jeju volcanic island. *Tectonics* 31 (4), TC4005. <http://dx.doi.org/10.1029/2011tc003092>.
- Sokolov, S.D., Bondarenko, G.Y., Morozov, O.L., Shekhovtsov, V.A., Glotov, S.P., Ganelin, A.V., Kravchenko-Berezhnoy, I.R., 2002. South Anyui suture, northeast Arctic Russia: Facts and problems. *Geol. Soc. Am. Spec. Pap.* 360, 209–224.
- Stixrude, L., Lithgow-Bertelloni, C., 2012. Heterogeneity in the mantle. *Annu. Rev. Earth Planet. Sci.* 40, 569–595. <http://dx.doi.org/10.1146/annurev.earth.36.031207.124244>.
- Syracuse, E.M., Abers, G.A., 2006. Global compilation of variations in slab depth beneath arc volcanoes and implications. *Geochim. Geophys. Geosyst.* 7 (Q05017). <http://dx.doi.org/10.1029/2005GC001045>.
- Tang, Y., Obayashi, M., Niu, F., Grand, S.P., Chen, Y.J., Kawakatsu, H., Tanaka, S., Ning, J., Ni, J.F., 2014. Changbaishan volcanism in northeast China linked to subduction-induced mantle upwelling. *Nat. Geosci.* 7, 470–475. <http://dx.doi.org/10.1038/ngeo2166>.
- Tatsumi, Y., Nakano, S., 1984. Lateral variation of K/Hf ratios in Quaternary volcanic rocks of Northeastern Japan. *Geochem. Jour.* 18 (6), 305–314. <http://dx.doi.org/10.2343/geochemj.18.305>.
- Tatsumi, Y., Sakuyama, M., Fukuyama, H., Kushiro, I., 1983. Generation of arc basalt magmas and thermal structure of mantle wedge in subduction zones. *J. Geophys. Res.* 88, 5815–5825.
- Tatsumi, Y., Shukuno, H., Yoshikawa, M., Chang, Q., Sato, K., Lee, M.W., 2004. The petrology and geochemistry of volcanic rocks on Jeju island: plume magmatism along the Asian continental margin. *J. Petrol.* 46 (3), 523–553.
- Tu, K., Xie, G.H., Zhang, M., Wang, J.W., Flower, M.F.J., Carlson, R.W., 1992. Sr, Nd and Pb isotopic compositions of Cenozoic basalt in East China. In: Liu, R.X. (Ed.), *Cenozoic Basalt in China: Geochronology and Geochemistry*. Seismology Press, Beijing, pp. 330–338.
- Wada, I., Wang, K., 2009. Common depth of slab-mantle decoupling: reconciling diversity and uniformity of subduction zones. *Geochem. Geophys. Geosyst.* 10 (Q10009). <http://dx.doi.org/10.1029/2009GC002570>.
- Wang, Q., Wyman, D.A., Xu, J.-F., Zhao, Z.-H., Jian, P., Xiong, X.-L., Bao, Z.-W., Li, C.-F., Bai, Z.-H., 2006. Petrogenesis of Cretaceous adakitic and shoshonitic igneous rocks in the Luzong area, Anhui Province (eastern China): Implications for geodynamics and Cu-Au mineralization. *Lithos* 89 (3–4), 424–446.
- Wei, W., Xu, J., Zhao, D., Shi, Y., 2012. East Asia mantle tomography: new insight into plate subduction and intraplate volcanism. *J. Asian Earth Sci.* 60, 88–103. <http://dx.doi.org/10.1016/j.jseas.2012.08.001>.
- Williams, S.E., Müller, R.D., Landgrebe, T.C.W., Whittaker, J.M., 2012. An open-source software environment for visualizing and refining plate tectonic reconstructions using high-resolution geological and geophysical data sets. *GSA Today* 22 (4/5).
- Wolbern, I., Jacob, A.W.B., Blake, T.A., Kind, R., Li, X., Duennbier, F., Weber, M., 2006. Deep origin of the Hawaiian tilted plume conduit derived from receiver functions. *Geophys. J. Int.* 166 (2), 767–781.
- Wu, F.-Y., Sun, D.-Y., Li, H., Jahn, B.-M., Wilde, S., 2002. A-type granites in northeastern China: age and geochemical constraints on their petrogenesis. *Chem. Geol.* 187 (1–2), 143–173.
- Wu, F.-Y., Lin, J.-Q., Wilde, S.A., Zhang, X.O., Yang, J.-H., 2005. Nature and significance of the early Cretaceous giant igneous event in eastern China. *Earth Planet. Sci. Lett.* 233 (1–2), 103–119.
- Xu, J.-F., Shinjo, R., Defant, M.J., Wang, Q., Rapp, R.P., 2002. Origin of Mesozoic adakitic intrusive rocks in the Ningzhen area of east China: partial melting of delaminated lower continental crust? *Geology* 30 (12), 1111–1114.
- Yamamoto, M., Morgan, J.P., 2009. North Arch volcanic fields near Hawaii are evidence favouring the restite-root hypothesis for the origin of hotspot swells. *Terra Nova* 21 (6), 452–466. <http://dx.doi.org/10.1111/j.1365-3121.2009.00902.x>.
- Yoo, H.J., Herrmann, R.B., Cho, K.H., Lee, K., 2007. Imaging the three-dimensional crust of the Korean peninsula by joint inversion of surface-wave dispersion and teleseismic receiver functions. *Bull. Seismol. Soc. Am.* 97 (3), 1002–1011. <http://dx.doi.org/10.1785/0120060134>.
- Yuan, X., Ni, J., Wang, Y., Wu, Y., Bina, C., Jin, Z., Dong, S., 1997. Lithospheric and upper mantle structure of southern Tibet from a seismological passive source experiment. *J. Geophys. Res.* 102, 27491–27500.
- Zhao, D., Hasegawa, A., Horikoshi, S., 1992. Tomographic imaging of P and S wave velocity structure beneath northeastern Japan. *J. Geophys. Res.* 97 (B13), 19909–19928.
- Zhao, D.P., Lei, J.S., Tang, R.Y., 2004. Origin of the Changbai intraplate volcanism in Northeast China: Evidence from seismic tomography. *Chin. Sci. Bull.* 49, 1401–1408.
- Zhao, D., 2012. Tomography and dynamics of western-Pacific subduction zones. *Monogr. Environ. Earth Planets* 1 (1), 1–70. <http://dx.doi.org/10.5047/meep.2012.00101.0001>.
- Zhang, M., Menzies, M.A., Suddaby, P., Thirlwall, M.F., 1991. EM1 signature from within the post-Archaean subcontinental lithospheric mantle: isotopic evidence from the potassic volcanic rocks in NE China. *Geochem. J.* 25, 387–398.
- Zheng, Y., Shen, W., Zhou, L., Yang, Y., Xie, Z., Ritzwoller, M.H., 2011. Crust and uppermost mantle beneath the North China Craton, northeastern China, and the Sea of Japan from ambient noise tomography. *J. Geophys. Res.* 116 (B12312). <http://dx.doi.org/10.1029/2011JB008637>.
- Zheng, Y.-F., Xiao, W.-J., Zhao, G., 2013. Introduction to tectonics of China. *Gondwana Res.* 23, 1189–1206. <http://dx.doi.org/10.1016/j.gr.2012.10.001>.
- Zhou, X.H., Armstrong, R.L., 1982. Cenozoic volcanic rocks of eastern China—secular and geographic trends in chemistry and strontium isotopic composition. *Earth Planet. Sci. Lett.* 58, 301–329.
- Zhu, L., Kanamori, H., 2000. Moho depth variation in southern California from teleseismic receiver functions. *J. Geophys. Res.* 105 (B2), 2969–2980. <http://dx.doi.org/10.1029/1999JB900322>.